FACULTY OF INFORMATION TECHNOLOGY AND ELECTRICAL ENGINEERING

Heshani Niyagama Gamage

WAVEFORMS AND CHANNEL CODING FOR 5G

Master's Thesis
Degree Programme in Wireless Communications Engineering
March 2017

Niyagama Gamage H. (2016) Waveforms and Channel Coding for 5G. University of Oulu, Faculty of Information Technology and Electrical Engineering, Department of Communications Engineering. Master's thesis, 63 p.

ABSTRACT

The fifth generation (5G) communication systems are required to perform significantly better than the existing fourth generation (4G) systems in data rate, capacity, coverage, latency, energy consumption and cost. Hence, 5G needs to achieve considerable enhancements in the areas of bandwidth, spectral, energy, and signaling efficiencies and cost per bit. The new radio access technology (RAT) of 5G physical layer needs to utilize an efficient waveform to meet the demands of 5G. Orthogonal frequency division multiplexing (OFDM) is considered as a baseline for up to 30 GHz. However, a major drawback of OFDM systems is their large peak to average power ratio (PAPR). Here in this thesis, a simple selective-mapping (SLM) technique using scrambling is proposed to reduce the PAPR of OFDM signals. This technique selects symbol sequences with high PAPR and scrambles them until a PAPR sequence below a specific threshold is generated. The computational complexity of the proposed scheme is considerably lower than that of the traditional SLM. Also, performance of the system is investigated through simulations and more than 4.5 dB PAPR reduction is achieved.

In addition, performance of single carrier waveforms is analyzed in multiple-input multiple-output (MIMO) systems as an alternative to OFDM. Performance of a single carrier massive MIMO system is presented for both uplink and downlink with single user and multiple user cases and the effect of pre-coding on the PAPR is studied. A variety of channel configurations were investigated such as correlated channels, practical channels and the channels with errors in channel estimate.

Furthermore, the candidate coding schemes are investigated for the new RAT in the 5G standard corresponding the activities in the third generation partnership project (3GPP). The schemes are evaluated in terms of block error rate (BLER), bit error rate (BER), computational complexity, and flexibility. These parameters comprise a suitable set to assess the performance of different services and applications. Turbo, low density parity check (LDPC), and polar codes are considered as the candidate schemes. These are investigated in terms of obtaining suitable rates, block lengths by proper design for a fair comparison. The simulations have been carried out in order to obtain BLER / BER performance for various code rates and block lengths, in additive white Gaussian noise (AWGN) channel. Although polar codes perform well at short block lengths, LDPC has a relatively good performance at all the block lengths and code rates. In addition, complexity of the LDPC codes is relatively low. Furthermore, BLER/BER performances of the coding schemes in Rayleigh fading channels are investigated and found that the fading channel performance follows a similar trend as the performance in the AWGN channel.

Keywords: 5G, RAT, OFDM, Channel coding, Polar, LDPC, Turbo, eMBB

TABLE OF CONTENTS

FOREWARD

This thesis is focused on energy efficient waveforms and channel coding schemes for 5G New Radio air-interface as a part of the 5Gto10G project at the Center for Wireless Communications (CWC) of University of Oulu, Finland. I express my sincere gratitude to my supervisor and mentor Prof. Nandana Rajatheva for his support and guidance throughout my period of masters studies. Also I express my gratitude to Prof. Matti Latva-aho, the head of the RAT group of CWC for his guidance. Also, I thank Dr. Pekka Pirinen, the project manager and the other colleagues of 5Gto10G project for their support in my research.

Also, I thank my parents and my siblings for their immense support in my life. Finally, I thank my dear husband Udaranga for for his endless support.

ABBREVIATIONS

Acronyms

1G	First Generation
2G	Second Generation
3G	Third Generation
3GPP	Third Generation Partnership Project
4G	Fourth Generation
5G	Fifth Generation
AR	Augmented Reality
AWGN	Additive White Gaussian Noise
BER	Bit Error Rate
BLER	Block Error Rate
BS	Base Station
CCDF	Complementary Cumulative Distribution Function
CDMA	Code Division Multiple Access
CRC	Cyclic Redundancy Check
CRCA-SCL	CRC Aided Successive Cancellation List decoding
CSI	Channel State Information
CSIT	CSI at the transmitter
DAB	Digital Audio Broadcasting
DFT	Discrete Fourier Transform
DVB-T	Terrestrial Digital Video Broadcasting
eMBB	Enhanced Mobile Broadband
Exp	Exponential Correlation
FDMA	Frequency Division Multiple Access
FFT	Fast Fourier Transform
FHD	Full High Definition
GFDM	Generalized Frequency Division Multiplexing
GOFDM	Generalized Orthogonal Frequency Division Multiplexing
IFFT	Inverse Fast Fourier Transform
IMT-Advanced	International Mobile Telecommunications-Advanced
IP	Internet Protocol
ISI	Inter Symbol Interference
LDPC	Low Density Parity Check
LTE	Long Term Evolution
M2M	Machine to Machine Communication
MAC	Medium Access Control
MBB	Mobile Broadband
MIMO	Multiple-Input Multiple-Output
mMTC	Massive Machine-Type Communications
NR	New Radio
OFDM	Orthogonal Frequency Division Multiplexing
OMS	Offset Min-Sum
PA	Power Amplifier
PAPR	Peak-to-Average Power Ratio

PDP	Power Delay Profile
PHY	Physical Layer
PSK	Phase Shift Keying
PTS	Partial Transmit Sequence
QAM	Quadrature Amplitude Modulation
QC	Quasi Cyclic
QPSK	Quadrature Phase Shift Keying
RAT	Radio Access Technologies
RF	Radio Frequency
SC	Successive Cancellation
SC-FDMA	Single Carrer - Frequency Division Multiple Access
SCL	Successive Cancellation List decoding
SLM	Selective Mapping
TBCC	Tail Biting Convolutional Codes
TDMA	Frequency Division Multiple Access
ULA	Uniform Linear Array
URLLC	Ultra-Reliable Low-Latency Communications
UT	User Terminal
VR	Virtual Reality
WLAN	Wireless Local Area Network

Symbols

$\mathbf{a}$	Exponential correlation coefficient
$\mathbf{D}_l$	Vector of PDPs of all the users
D	Length of ULA array
d	distance from the m_o antenna to the m^{th} antenna in ULA array
d_c	Average check degree
d_l	Power delay profile
d_v	Average variable degree.
E_b	Bit energy
Ec	Symbol power
f_k	k^{th} subcarrier
$\mathbf{H}$ $[l]$	Fading channel coefficients matrix of the l^{th} path
I	Number of iterations
K	Number of users
L	Number of channel taps -1
L_s	Oversampling factor
L_p	List size of the SCL decoder
M	Number of receive antennas at the base station
M_a	Alphabet size
M_b	Memory length
N_o	Noise power spectral density
N_s	Number of sub carriers
N_b	Coded block length

P	Scrambler polynomial
P_b	Number of parity bits
R	Code rate
S	Length of the scrambler polynomial
T	Symbol period
$\mathbf{t}$	Exponential correlation matrix of a channel
Th	Threshold value
U	Number of scramblers
$\mathbf{w}\left[\mathbf{n}\right]$	Additive white noise vector
$\mathbf{X}$	Transmit signal vector
$\underline{\mathbf{X}}$	Block of data symbol
$\mathbf{x}\left[\mathbf{n}\right]$	Transmitted signal
X_k	k^{th} data symbol
x_{rms}	Root mean square value of waveform x
$x(t)$	OFDM signal at time t
$\mathbf{Y}$	Received signal vector
$\mathbf{y}\left[\mathbf{n}\right]$	Received signal
$\mathbf{W}$	AWGN vector
Δf	Subcarrier space
ϵ	Estimation error
λ	Threshold in decibels
λ_l	PAPR of the lowest PAPR sequence
ρ	Antenna spatial correlation
σ^2	Variance

Operators

$\left\|\cdot\right\|$	Absolute value
$E\left[\cdot\right]$	Expected value
$J_0(\cdot)$	Zeroth order Bessel function of the first kind
$log_2(\cdot)$	Logarithm of base 2
$\sum$	Summation operation

1. INTRODUCTION

Services offered by cellular communication systems have evolved from the first generation(1G) to the fourth generation (4G) adding further enhanced services in each generation. 1G was only for voice calls followed by the second generation (2G), which added text messaging services. The third generation (3G) added mobile internet services to 2G. Currently 4G offers high capacity mobile multimedia service at 1 Gbps data rate when stationary and 100 Mbps rate when mobile, making it 250 times better than the 3G services. 5G New Radio (NR) is the forthcoming evolution of mobile technology expected to be in use by the year 2020 with a wide range of usability beyond the uses of 4G [1]. Performance parameters of 5G technologies are expected to be tens and thousands times better than in 4G. Although the performance parameters for 5G are not standardized yet, typical parameters [2] are stated in Table 1 with 4G international mobile telecommunications-advanced (IMT-Advanced) performance parameters for reference.

Table 1: Suggested performance parameters for 5G.

Parameter	5G suggested Performance	IMT-Advanced Performance
Network capacity	10 000 times the capacity of current network	2.2 downlink and 1.4 uplink (bps/Hz/cell)
Peak data rate	10 Gbps	3 Gbps Downlink and 1.5 Gbps Uplink
Latency	Less than 1 ms	10 ms
Peak spectral Efficiency	2/3/5 x greater than IMT-Advanced	6.75 bps/Hz

Furthermore, low energy consumption as well as cost are also desired. In addition 5G should enable machine to machine communication (M2M) at ultra low cost and ultra high reliability while supporting 10 years battery life. To facilitate these needs spectral efficiency, signaling efficiency, bandwidth and coverage should be significantly enhanced compared to 4G.

Number of mobile devices such as mobile phones, tablets and smart watches has been exponentially increasing in the last few years and at the same time more and more applications such as video streaming/downloading, multi-player gaming which requires a large bandwidth are emerging. In addition more and more household items such as fridges, ovens, heating systems, and even clothes are being developed as "smart devices" which can be connected with other devices via internet. Majority of these require a small amount of data to be transferred between the devices in a large network. The networks like these, called Internet of Things (IoT) are increasing adding different kind of devices in household as well as industrial environments. Current mobile networks should be enhanced by several factors in terms of capacity, data rate, latency and

other performance aspects in order to facilitate the increasing demand through above mentioned technologies.

Therefore the two most significant use cases, which are the main drivers of the development of 5G network technology can be recognized as [3]

1. ***Mobile broadband (MBB) services.***
   MBB is the term used for wireless internet access through modems and other mobile devices. MBB was the primary drive of the 4G and it will remain the most critical use case of 5G. As the current networks provide faster data speeds, many data intensive applications are emerging for both business and consumer use. At present, a large percentage of the MBB users is for video streaming and downloading. As higher resolution videos like 4K becomes more common, 4G networks will not be able to cope up with a large number of users at the same time. In addition the growing use of cloud services will add more traffic to demand for MBB. Furthermore virtual reality (VR), augmented reality (AR), multi-player gaming are some other content-rich services which are expected to be increasing the demand for better MBB services. All of these services are content-rich and at the same time number of devices accessing these services are increasing. By the nature of these applications, they have a large volume of data the latency must be low to have a better user experience, these users need faster, higher-capacity networks that can deliver content-rich services.

2. ***Internet of things(IoT)***
   IoT is a network of interconnected devices, such as household appliances, industrial machinery, vehicles, medical devices, environmental sensors and etc embedded with sensors and actuators, that are provided with unique identifiers and the ability to compute, coordinate and communicate, data over a network without requiring human intervention. There are two varieties of IoT applications based on the nature of communication between the devices. They are

   (a) Massive machine type communication (mMTC)
   These are networks of large number of low cost, low power devices which require infrequent transferring of a very small amount of data which are not delay-sensitive. Some of the examples of these kind of systems are wireless sensor networks, smart homes, smart cities etc. These networks needs to be scalable, so users can add more and more devices to the network.

   (b) Mission critical communication
   In this scenario machine-to-machine communication needs to be ultra-reliable with low latency. Usually these devices are relatively expensive. Example scenarios are autonomous vehicles, remote surgeries, and industry automation. These applications needs extreme reliability and low latency to ensure human safety.

Based on different user requirements, new radio access technology for 5G systems includes three scenarios; namely,

1. ***Enhanced Mobile Broadband (eMBB).***
   This is being developed to deliver a better MBB services in 5G with higher data

rates, higher capacity and better user experience. This is the most profitable area in 4G and the eMBB remains the most critical scenario for 5G as well because the ongoing growth of users demanding the eMBB services proves to be strong and profitable. 5G is expected to deliver 10 Gbps peak throughput and up to 10,000 times the current network capacity. Based on its requirements, eMBB needs to support a much wider range of code rates, code lengths and modulation orders than LTE. In the current assumption, eMBB code lengths range from 100 to 8000 bits (optionally $12,000 - 64000$ bits) and code rate ranges from $1/5$ to $8/9$.

2. ***Massive machine type communications (mMTC).***
   This scenario is being developed to cater the massive-machine networks to enable IoT at home and in business. Very low power consumption, low cost, ability to handle a large number of connections and good scalability are desired in these type of systems.

3. ***Ultra reliable low latency communications (URLLC).***
   This is being developed to cater mission critical communication needs with ultra-reliability and low latency.

In order to cater for the requirements of these scenarios, 5G needs to to achieve significant enhancements in addition to existing technologies. Some of the main technologies under research to achieve the data rate and capacity for 5G are [4]:

1. Densification of Networks
   Utilization of more base stations in a heterogeneous network which is a combination of macro cells in order to increase the capacity. By reducing the cell size we can obtain a higher overall effective use of the available spectrum. This will require efficient interference cancellation methods and other techniques to ensure that small cells in the macro-network and deployed as femtocells can operate satisfactorily are required.

2. Increased bandwidth
   This includes additional bandwidth added to the mobile networks and increasing spectral efficiency. This will enable the networks to cater for more traffic and devices. Currently spectrum of the wireless communications are limited to 6GHz. To increase the capacity, spectrum above 10GHz up to 100 GHz will be added to the spectrum of the network. This will need developments in millimeter wave technologies and other high frequency communication technologies. In addition efficient spectrum sharing and cognitive radio will enable higher efficiency in spectrum usage.

3. Increased spectral efficiency
   Massive MIMO is a area under research for enhancing spectral efficiency.

4. New air interface
   This includes waveforms, multiplexing schemes, modulation schemes and coding schemes to reduce the latency in the air-link, and to increase spectral efficiency, connection density, throughput, area capacity density and energy efficiency.

This thesis is focused on technologies for the new air-interface, waveforms and coding schemes for the 5G NR PHY Layer. In Chapter 2, some of the technologies available for waveforms and coding scheme are discussed. In the third chapter, a low complex algorithm is proposed to reduce the PAPR of the OFDM waveforms followed by single carrier waveform performance evaluation the the fourth chapter. Candidate coding schemes for the new air-interface of 5G are evaluated in the fifth chapter. Conclusions and future recommendations are given in the final two chapters.

2. BACKGROUND AND LITERATURE

In this chapter the basic concepts and available literature of the waveforms and coding schemes are discussed. In the first section we focus on the available waveform techniques for energy efficient waveforms. We discuss about the performance aspects of OFDM waves and single carrier waves. Next we discuss about coding schemes for 5G eMBB scenario.

2.1. Energy Efficient Waveforms

The waveform will be a key specification of the wireless standard and will have a major effect on the performance parameters. Wave forms used in each generation are listed in the Table 2.

Table 2: PHY / MAC for each generation.

Generation	Waveforms
1G	Analog - FDMA
2G	Digital FDMA/TDMA
3G	CDMA
4G	OFDM, FDMA/TDMA

In this thesis performance aspects of OFDM waveforms and single carrier waveforms are investigated.

2.1.1. OFDM waveforms

OFDM is a multi-carrier modulation technique where the signal is constructed from a number of closely spaced modulated sub-carriers. OFDM is being used in several high data rate wireless systems due to many advantages it provides including;

1. Resilience to multipath fading, inter-symbol interference (ISI), co-channel interference and impulsive parasitic noise, due to multiple narrow band sub channels with a lower data rate on each sub channel.

2. Lower implementation complexity compared with the single carrier solution with usage of fast Fourier transform (FFT)/Inverse FFT (IFFT) blocks.

3. High spectral efficiency due to usage of closely spaced overlapping subcarriers.

Therefore, OFDM has been adopted in many wireless standards such as wireless local area network (WLAN) radio interfaces IEEE 802.11a, g, n, ac, digital audio broadcasting (DAB), and terrestrial digital video broadcasting (DVB-T). Also OFDM has already been adopted as a radio access scheme for several of the latest cellular network and mobile broadband standard specifications such as WiMax and 3GPP LTE 4G mobile broadband standard. In 4G LTE, OFDM with modulated data directly mapped to sub-carriers is used only in downlink transmission in the form of OFDM multiple access. In the uplink, data is first transformed via a discrete Fourier transform (DFT) before being modulated and transmitted via sub-carriers in the form of single carrier frequency division multiple access (SC-FDMA) due to the PAPR problem.

Waveform

We consider an OFDM system with N_s subcarriers. Let $\underline{\mathbf{X}} = [X_k; k = 0, 1, \ldots, N_s - 1]$ be a block of N_s data symbols drawn from an alphabet of size M_a. Each of these symbols will modulate one in a set of N_s orthogonal subcarriers $[f_k, k = 0, 1, \ldots, N_s - 1]$ where $f_k = k\Delta f$, $\Delta f = 1/N_s T$, and T is original symbol period. The complex envelope of the transmitted signal $x(t)$ can be written as

$$x(t) = \frac{1}{N_s} \sum_{k=0}^{N_s-1} X_k e^{j2\pi f_k t} \quad ; 0 \leq t < N_s T. \tag{1}$$

Peak-to-average power ratio (PAPR)

If $|x|_{peak}$ and x_{rms} are peak value and root mean square value of waveform x respectively, then PAPR of the waveform x can be defined as

$$PAPR\{x\} = \frac{|x|_{peak}}{x_{rms}}. \tag{2}$$

To better approximate the PAPR of continuous time OFDM signals, OFDM samples are taken by L_s times oversampling. [5]. Oversampled FFT output $x\,[n]$ will be

$$x\,[n] = \frac{1}{\sqrt{N_s}} \sum_{k=0}^{N_s-1} X_k e^{j\frac{2\pi nk}{L_s N_s}} \quad ; 0 \leq n < L_s N_s - 1. \tag{3}$$

PAPR of the OFDM signal is defined as

$$PAPR\{x\,[n]\} = \frac{\max_{0 \leq n \leq N_s L_s} [|x\,[n]\,|^2]}{E\,[|x\,[n]\,|^2]}. \tag{4}$$

Complementary Cumulative Distribution Function (CCDF)

CCDF for PAPR is the probability of OFDM symbols with PAPR exceeding some threshold λ. Depicted in Fig. 1 is CCDF plots of 4 times oversampled OFDM PAPR for N subcarriers. It can be seen that PAPR increases as the number of subcarriers increases. For a small number of N, the probability that the PAPR of the OFDM signal exceeds a certain threshold λ is given by [6]

$$Pr\{PAPR > \lambda\} = 1 - (1 - e^{-\lambda})^{N_s}. \tag{5}$$

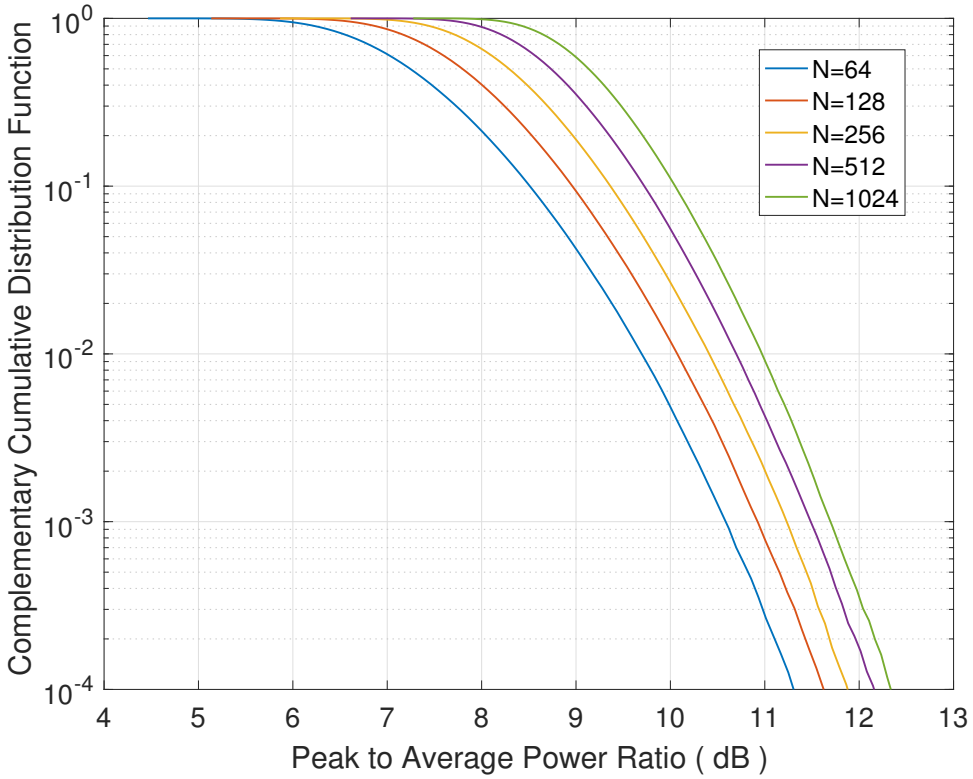

Figure 1: CCDF of PAPR in 4 times over sampled OFDM system with N subcarriers.

High PAPR in original OFDM signals will lead to distortion of the signal if the transmitter has nonlinear components such as power amplifiers (PAs). Nonlinear devices will cause spectral spreading, inter modulation and constellation distortion. To avoid this, usage of expensive high power amplifiers in a very large linear range, approximately equal to the dynamic range of the OFDM signal is required. Also high PAPR signals prevent PA from operating in a near saturation region reducing the PA efficiency. There are several alternative waveforms being proposed to avoid the disadvantages of OFDM. They are time–frequency packing, nonorthogonal Signals, filterbank multicarrier, generalized frequency division multiplexing (GFDM) and tunable OFDM.

Many different techniques have been proposed to reduce PAPR problem. The simplest and the most used technique is clipping and filtering [7], [8]. However, this method introduces signal distortion resulting in-band noise and out-of-band leakage, which leads to BER degradation. Coding schemes such as block coding [9], cyclic coding [10] and complement block coding [11] can also be used to reduce PAPR. However, PAPR reduction capability of these schemes is limited to OFDM systems with small number of subcarriers and there is a data rate loss and a high computational complexity. Partial transmit sequence (PTS) [12], [13] is a probabilistic scheme to reduce PAPR. It carries a high computational complexity due to the calculation of PAPR value at each step of the optimization algorithm. Also, this technique results in a BER degradation and a data rate loss. Tone reservation and tone injection [14] are efficient techniques, which reduce the PAPR by reserving a subset of tones for generating PAPR reduction

signals. These techniques, however, have a limited PAPR reduction capability, high complexity, data rate loss and a power increase. Nonlinear companding, mainly μ-law and exponential companding [15] are effective techniques for PAPR reduction. Especially exponential companding is an attractive method due to its simplicity and very high PAPR reduction capability by minimizing the dynamic range of the OFDM signal. We found out through simulations that this method has a poor BER performance due to amplification of noise at the receiver. Generalized OFDM (GOFDM) [16] is a recent method, which lowers PAPR by reducing the number of subcarriers within OFDM symbols. Although it produces significantly low PAPR, there are major drawbacks such as high computational burden and the requirement of perfect knowledge of channel transfer function etc.

Selective Mapping (SLM) technique is a probabilistic scheme, where U different OFDM signals are generated as candidates for a specific signal and then one with the lowest PAPR is selected for the actual transmission. At the receiver, it is necessary to know which one of U candidates is transmitted. Hence transmission of side information is needed in conventional methods resulting a data rate loss. There are several techniques that has been proposed to generate different OFDM signals including, phase rotation [17] and turbo coding [18]. Usually, complexity of SLM method is very high due to its requirement of calculating $U \times N$ IFFTs whenever SLM is applied for an OFDM system with N subcarriers.

Apparently none of these techniques have all the desired features of a OFDM system including;

1. Large PAPR reduction.
2. Low computational complexity.
3. No degradation in BER Performance.
4. Low average power and no requirement of additional transmit power.
5. No bandwidth expansion or spectral spillage.

All of the above mentioned PAPR reduction techniques tend to compromise one or more of those wanted objectives in reducing BER. Hence research of PAPR reduction is still very intensive. A simple modified SLM technique using an array of scramblers to reduce the PAPR of OFDM signals [19] is discussed in the following chapter of this thesis. Unlike most of the schemes mentioned above, it has a simple architecture and does not have a BER degradation.

2.1.2. Single Carrier waveforms

Single carrier waveforms regain the interest recently. In 5G some filtered transmissions for the lower frequency region below 6 GHz are in the development of NR air interface [20]. Given the way 3GPP standardization is evolving massive MIMO is going to be a reality sooner rather than later [1, 21]. This also takes into account the fact that there will be new frequency ranges being explored in the mmWave range [22] where work is going on to develop new radio access technologies (RATs). One disadvantage

of a large number of antennas in a multi-carrier system will be the large number of IFFT/FFT blocks that will be needed. Given both these issues it will be good to have a system which can take advantage of the higher number of antennas being deployed in base stations. One direct implication from Marzetta's work [23] is that there is the possibility of a reduced complexity receiver utilizing the large dimension and hence realizable orthogonality due to that. It is also important to see the performance of such systems with closer to reality channel models. In our case some results are obtained using measured channels obtained by our CWC colleagues [24, 25].

The main reason why multi-carrier OFDM based system is universally adopted is due to the simplicity of the receiver implementation, which circumvents the need for sophisticated and complex equalization. With a single carrier system the issue of equalizer can be managed provided that one of the transmission link ends has a large number of antennas. Another practical thing to be dealt with given the large number of channels to be measured is the accuracy of the estimate. Attention must be paid therefore to have a realistic performance analysis.

A survey of single-carrier systems has been presented by Yang et. al. [26]. With the incorporation of MIMO methods in practical wireless systems, e.g., LTE, 4G, it has been possible to improve the link reliability and provide a higher capacity with better spectral efficiency. Moving further along this path there has been a tremendous amount of research in massive MIMO techniques. Marzetta [23] showed that it is possible to mitigate the effects of fast fading and uncorrelated receiver noise through orthogonality arising out of large dimensions of matrices due to the large number of antennas. Pitarokoilis et. al. [27] considered the application of single-carrier transmission in a large scale antenna system in the downlink, where they showed that the receiver side can essentially work without an equalizer. This effect is due to the properties as shown by [23]. The base station transmitter uses a pre-coding scheme matched to the frequency selective channel. Though single-carrier method here eliminates the use of an equalizer, it is worthwhile to analyze the effect on the PAPR. Sheng et. al. [28] investigated a single-carrier modulation uplink scheme for a Rician channel with maximum likelihood (ML) equalization expanding on [27]. A more detailed study is given in [29]. In the case of a Rayleigh fading channel the receiver will become simpler with a one tap equalizer similar to that used in an OFDM system. There has also been a lot of work for single-carrier schemes, which employ a cyclic prefix and frequency domain equalization [30]. Together with [26] therefore the literature on single-carrier systems has been gaining significant momentum.

As mentioned previously, there are several issues specific to downlink and uplink respectively. In the case of downlink with multiple RF chains for a large antenna system, it is prudent to have as distortion-less as possible signal for transmission since this has direct consequences to the spectral mask, which is tightly regulated. As the number of carriers increases this poses a considerable challenge in OFDM systems. If, however, this can be resolved with a single carrier scheme, which does not have the same PAPR properties it will be quite useful. Naturally, in this light the fundamental reason for preferring OFDM in the first place was the need for a simpler receiver with one tap equalize. While it can be shown that with a higher number of antennas the receiver of a single carrier system can still be less complex as opposed to a full fledged time domain equalizer needed in a frequency selective channel with multiple taps and a system employing high level modulation for increased bit rates, the performance of

such a system under less ideal conditions needs further investigation in order to bench mark against the traditional OFDM system.

2.2. Channel coding

Channel coding plays an important role in achieving higher data rate in order to have a fast and error free communication since data transmission occurs in an imperfect channel environment. The selected channel code must have an excellent BLER performance in a specific range of block lengths and code rates. Low computation complexity, low latency, low cost and higher flexibility are desired for the coding scheme. Furthermore, reduced energy per bit and improved area efficiency are required to support higher data rates. Tail biting convolutional codes (TBCC), turbo codes, LDPC codes and polar codes are the competing coding schemes considered as the candidates for 5G. However, TBCC is not considered for the eMBB scenario since it has a poor performance in large block lengths and low code rates. In the fifth chapter of this thesis, we review candidate error correction coding schemes for 5G eMBB scenario and evaluate their performances.

Although many coding schemes with capacity achieving performance at large block lengths are available, many of those do not show consistent good performance in a wide range of block lengths and code rates as the eMBB scenario demands. But turbo, LDPC and polar codes show promising BLER performance in a wide range of coding rates and code lengths and hence are being considered for 5G physical layer.

2.2.1. Turbo codes

Introduced in [31], turbo code encoder is built using a parallel concatenation of two recursive systematic convolutional codes and the associated decoder, using a feedback decoding rule. Due to the low error probability performance within a 1dB fraction from the the Shannon limit and relatively low complexity, turbo codes are being used in a variety of applications such as deep space communications, 3G/4G mobile communication in Universal Mobile Telecommunications System (UMTS) and Long Term Evolution (LTE) standards and Digital Video Broadcasting (DVB). Although it is being used in 3G and 4G, it may not satisfy the performance requirements of eMBB for all the code rates and block lengths as the implementation complexity is too high for higher data rates. In addition an error floor is observed in turbo code BER. In [32, Fig. 8.18] the error floor is at BER of 10^{-6}.

2.2.2. LDPC codes

LDPC codes were originally invented and published in [33] in 1962, they were not in use until it was rediscovered by Mackay [34] in 1997. He showed that the empirical performance of LDPC codes can approach the Shannon limit similar to turbo codes or even better. LDPC codes are linear codes and as the name suggests, has a sparse parity check matrix consisting low density $'1's$. Due to the sparsity of the parity check matrix,

LDPC codes have relatively simple and practical decoding algorithms. Decoding is done by iterative belief propagation decoding algorithms which estimates bit values and parity check values in bit and check nodes respectively and passing values between them in each iteration. The accuracy of the estimates will be improved in each iteration and the number of iterations is decided based on the requirement of the application. Trade-offs are possible between the bit error performance, latency and the complexity. Modern LDPC decoders work with soft decision algorithms which further enhance the decoder gain. Due to their excellent ability to achieve theoretical limits of channel capacity, LDPC codes are currently being used in many communication systems such as DVB-S2, 802.11n (Wi-Fi allowing MIMO) and 802.16e (Mobile WiMAX) etc.

Turbo codes and LDPC codes were competing against each other in various use cases and application as these codes both show good performance. Turbo codes generally have a low encoding complexity and high decoding complexity whereas LDPC codes have a high encoding complexity but low decoding complexity.

2.2.3. Polar codes

Polar codes were introduced by Arikan [35] in 2009 and they are the first provably capacity-achieving codes with low encoding and decoding complexities. Polar codes outperform turbo codes in large block lengths while no error flow is present. The concept behind channel polarization in polar codes is transforming N copies (transmissions) of the channel (e.g., say additive white Gaussian noise channel) with a symmetric capacity of $I(W)$ into extreme channels of capacity close to one or zero. Out of N channels, $I(W)$ fraction will become perfect channels and $1 - I(W)$ fraction of channels will become completely noisy channels. Then the information bits are sent only through good channels while inputs to other channels are made frozen into one or zero. The amount of channel polarization increases with the block length. Some of the issues with polar codes are, that the code design is channel independent hence not versatile for mobile fading channels and the limited application experience due to its immaturity. Polar codes have better energy-efficiency for large block lengths than other codes.

3. PAPR REDUCTION OF OFDM WAVEFORMS

In this section a low complex method to decrease the OFDM PAPR is suggested. The proposed technique is explained in Section 3.1 followed by the simulations of the high PAPR sequences scrambling scheme and analysis of the simulation results in Section 3.2.

3.1. System model

In SLM it is assumed that, U statistically independent alternative sequences, which represent the same information are generated by some suitable means. The sequence with the lowest PAPR is selected for transmission. The probability that the lowest PAPR λ_l exceeds a certain threshold λ is given by [17]

$$Pr\{\lambda_l > \lambda\} = (Pr\{PAPR > \lambda\})^U. \tag{6}$$

As stated in (6), if the threshold λ is set to a reasonable value, there is a significant number of symbol sequences with PAPR lower than the threshold after OFDM modulation. For example, if a system with $N = 128$ subcarriers is considered, from Fig. 1, it can be seen that about 85% of sequences will exceed a $7dB$ threshold and about 42% sequences will exceed an $8dB$ threshold. Hence doing a transformation to all the incoming symbol sequences is not necessary. Therefore a technique to reduce the PAPR of only the sequences exceeding a pre-set threshold is proposed rather than searching a minimum PAPR for all the sequences which will reduce the computational complexity significantly. A predefined array of U scramblers is used to change high PAPR sequences.

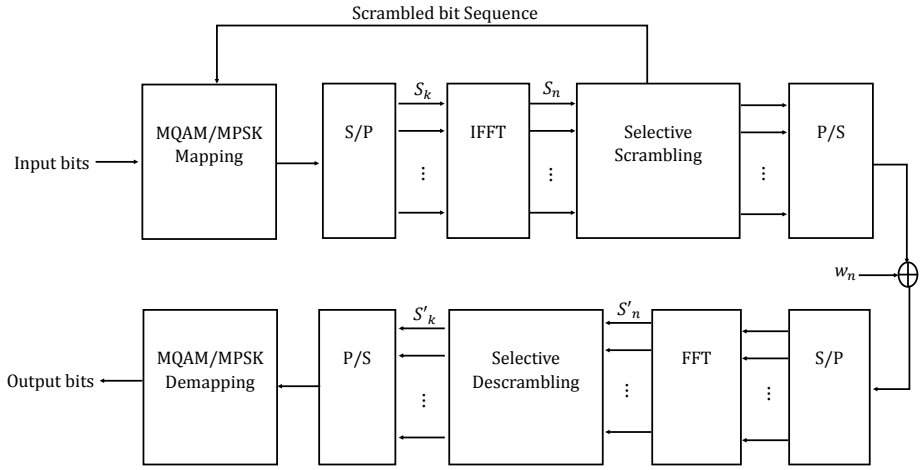

Figure 2: System model.

A block diagram of the proposed method is shown in Fig. 2 and the algorithm is given as Algorithm 1. In this method, PAPR of OFDM modulated symbol sequence

Algorithm 1 PAPR reduction algorithm

procedure PAPR REDUCTION
  $PAPR_{min} = \inf$,
  j = 0
  for each incoming symbol sequence d **do**
    QAM/QPSK modulation.
    OFDM modulation
    Oversampling and PAPR calculation
    if $PAPR_j < PAPR_{min}$ **then** $PAPR_{min} = PAPR_j$ and $j_{min} = j$
    end if
    if $PAPR_j >$Threshold **then**
      if Scrambler $j \leq$ Scrambler array length **then**
        Scramble the sequence using j^{th} scrambler
        $j++$,
        Goto step 3.
      else Transmit S_{min}, j_{min}
      end if
    else Transmit S_j , j
    end if
  end for
end procedure

is computed for each incoming symbol sequence and it is compared against a pre-set threshold value. If it exceeds the threshold value, the input symbol sequence is scrambled by a scrambler selected from the set of scramblers and PAPR for the new sequence is computed again. If PAPR drops below the threshold, the scrambling will be terminated and that sequence is transmitted with the index of the scrambler used in specific sequence for descrambling at the receiver. If the used scrambler does not make the PAPR to drop below the threshold, next scrambler from the array is used. This will be repeated until all the scramblers of the scrambler array are used. If it does not drops below the threshold, the sequence with minimum PAPR will be transmitted along with the corresponding scrambler index. If the original OFDM signal has a PAPR below the threshold, zero is sent as scrambler index. At the receiver, scrambler index is checked and if it is zero, no descrambling is used and signal is demodulated in the usual way. However, if the scrambling index is greater than zero, corresponding descrambler is used to descramble the signal before demodulation.

3.1.1. Scrambler and descrambler

A scrambler is used to convert the N length symbol sequence which is drawn from an alphabet of size M_a to a different S length sequence from the same alphabet. Models of scrambler and corresponding descrambler used in this technique are depicted in Fig. 3 and Fig. 4 respectively. They consist of S linear feedback shift registers. All adders are modulo M_a adders. Different scramblers of the same length can be defined by a

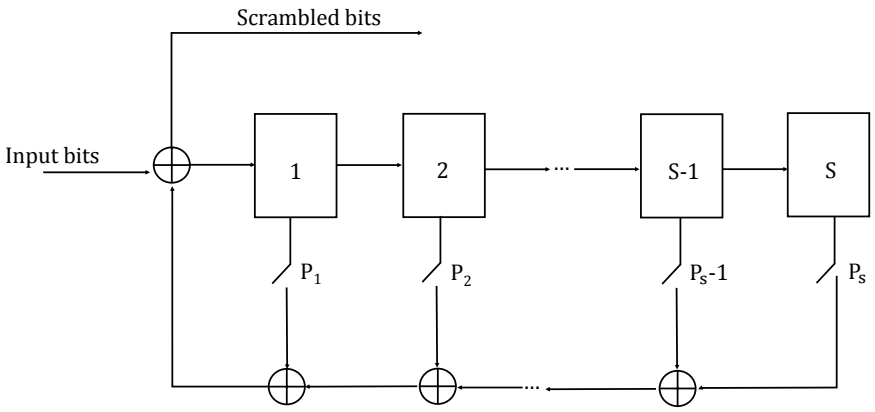

Figure 3: Scrambler for an S length sequence.

choosing different sequence of switches to be kept **ON** which is denoted by P_s. These scramblers can be defined by the scrambler polynomial P where,

$$P = [\,1\; P_1\; P_2\; \ldots\; P_S]\,; P_S \in \{1, 0\} for\; s = 1 \cdots S.$$

Proposed technique has a lower computational complexity than the SLM technique and will not have a BER degradation given that the scrambler index signal is decoded accurately. A simple repetition coding can be used to ensure accurate decoding of the scrambler index signal at the receiver. The subcarrier dedicated to scrambler side information will be the drawback of this system. However, the effect of this is insignificant when number of subcarriers used are high enough. Also there is a compromise between PAPR reduction and amount of side information needed to transmit the scrambler identification. For example, in quadrature amplitude modulation (QAM), if more than 3 scramblers are used, 2 subcarriers will be needed to send scrambler indices. In 16QAM, up to 15 scramblers can be used, with overhead of 1 subcarrier for side information. If more scramblers are used in order to have better PAPR reduction capability, more than one subcarrier will have to be dedicated for scrambler index signal, reducing spectral efficiency.

3.2. Simulations

In order to verify the performance of the high PAPR sequence scrambling in reduction of PAPR, a base band OFDM system as in Fig. 2 with the number of subcarriers $N = 128$ is considered throughout the computer simulations. The oversampling factor is L is set to 4. The randomly generated input data are modulated by $16QAM$. An array of $U = 15$ scramblers is used for PAPR reduction throughout the simulations, so that only one subcarrier is needed for side information.

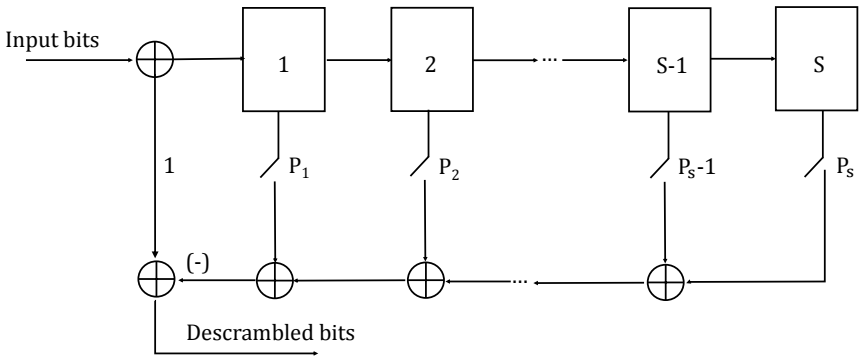

Figure 4: Descrambler for an S length sequence.

Fig. 5 has the CCDF curve of PAPR of the signal after applying proposed technique with threshold $Th = 8dB$. It is compared with PAPR curve of the original OFDM. It can be observed that this method is able to contain maximum PAPR value below $8dB$ with $8dB$ is set as threshold and there is more than $4dB$ PAPR reduction from original OFDM signal in this instant.

Fig. 6 depicts the usage of scramblers by symbol sequences. Zero means no scrambler is used. Although 15 scramblers are used in this case, it can be seen from the histogram that

- More than 58% of the sequences do not need any scrambler.
- About another 25% of signals go below threshold after the 1st scrambler.
- About 10% more of signals get below threshold after 2 scramblers.
- Another $4{,}3\%$ of signals go below threshold after 3 scramblers.
- Only $0{,}4\%$ sequences need more than 5 scramblers.
- less than $0{,}007\%$ sequences have to use more than 10 scramblers to achieve PAPR below threshold.

Therefore, it is clear that this technique reduces the computational complexity of the original SLM technique as it does not need to compute all K candidate sequences and choose the optimum.

Fig.7 has the CCDF curve of PAPR of the signal after applying proposed technique with threshold reduced to $Th = 7dB$. Again it is compared with PAPR curve of the original OFDM. It can be seen that the maximum PAPR value reaches about 7.8 dB at 10^{-5} CCDF exceeding the threshold of 7 dB. From the histogram in the Fig. 8, it can be seen that only about 13% of the original sequences are below the given threshold

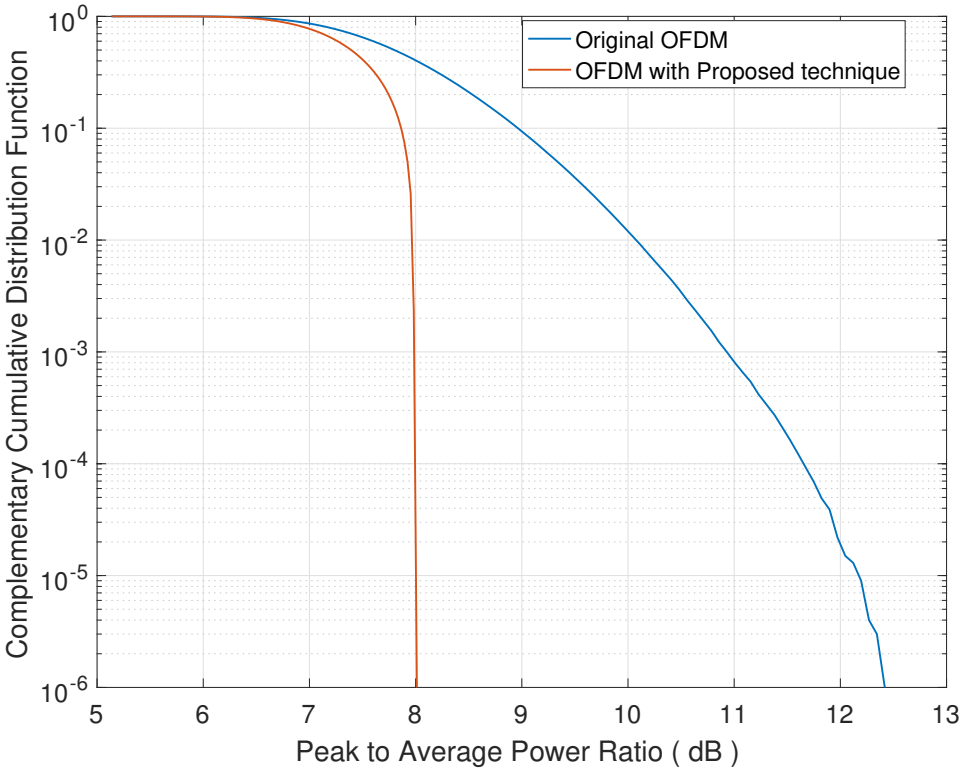

Figure 5: PAPR comparison of OFDM and the proposed technique, 128 subcarriers with 8 dB threshold and 15 scramblers.

and there are sequences which have a PAPR value above the threshold even after using all the scramblers. For those sequences, the sequence which gives the minimum PAPR output of all scrambled and non-scrambled sequences will be used for transmission. Thus at this threshold, computational complexity is increased from the previous instant when $Th = 8dB$, but, it still is lower compared to SLM. The drawbacks of this method are reduction in spectral efficiency associated with the side information overhead and the time delay in selecting the most suitable scrambler for the particular sequence. These drawbacks can be minimized by setting the threshold to a suitable value and using a small number of scramblers. This can be a trade off among the amount of PAPR reduction, computational complexity and side information overhead.

Fig. 8 shows the evaluation of the PAPR reduction capability of the proposed method, when the number of subcarriers is increased. The threshold value Th is changed according to the number of subcarriers so that computational complexity does not increase. Table 3 has a comparison of the proposed method with three other typical PAPR reduction techniques.

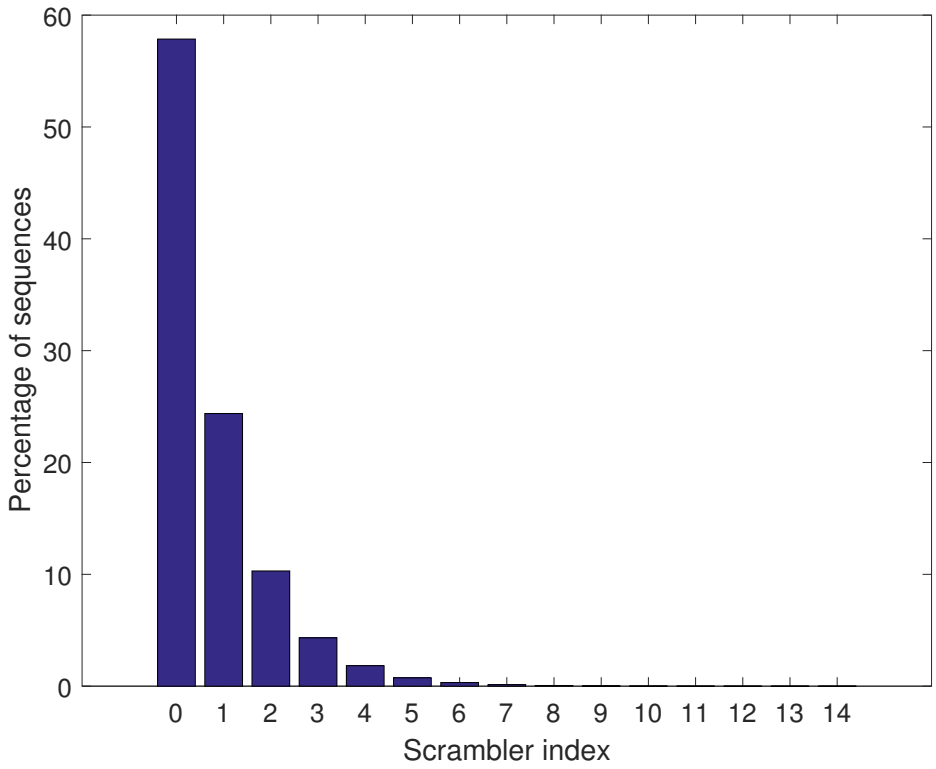

Figure 6: Percentage of sequences which has used each scrambler for $Th = 8dB$. Zero means no scrambler is used.

Table 3: Comparison of PAPR reduction techniques.

PAPR reduction technique	PAPR reduction capability	Implementation complexity	Data rate loss	BER degradation
Clipping& Filtering	$\leq 3dB$	Low	No	Yes
SLM	$\leq 4dB$	High	Yes	No
PTS	$\leq 4dB$	High	Yes	No
Proposed Method	$\leq 4{,}5dB$	Low	Yes	No

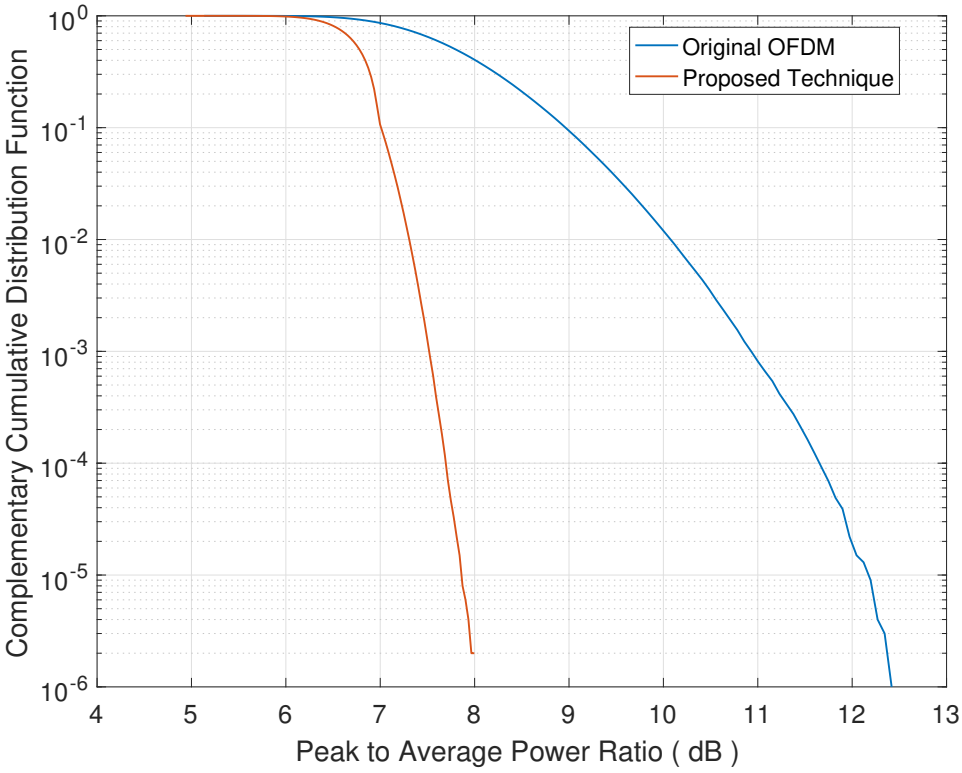

Figure 7: PAPR comparison of OFDM and the proposed technique, 128 subcarriers with $7dB$ threshold and 15 scramblers.

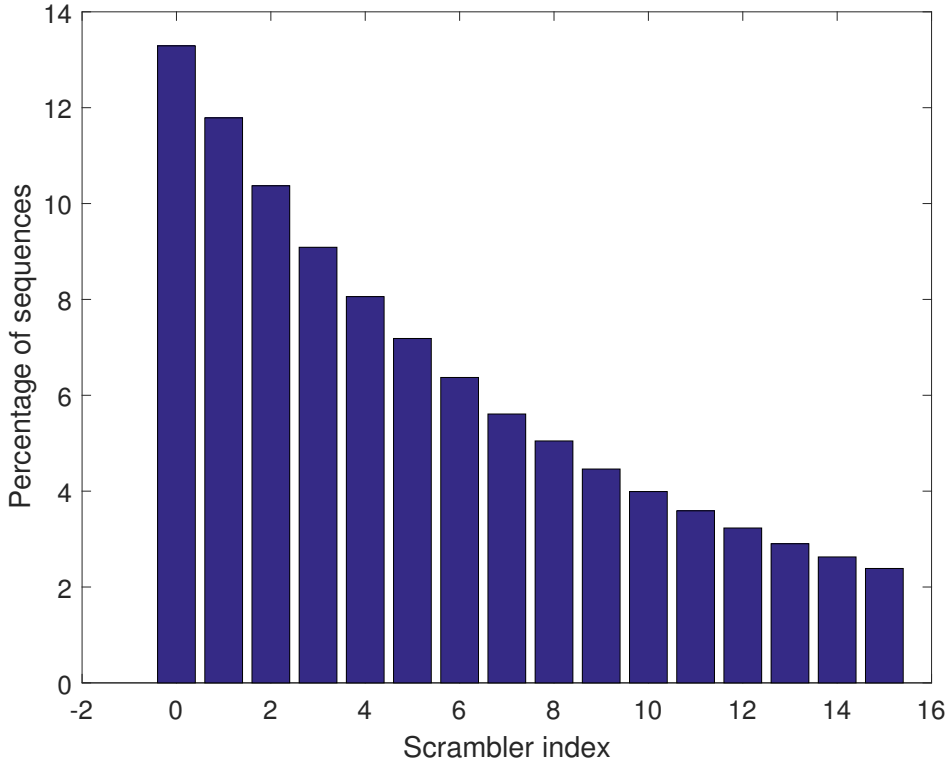

Figure 8: Percentage of sequences which has used each scrambler for $Th = 7dB$. Zero means no scrambler is used.

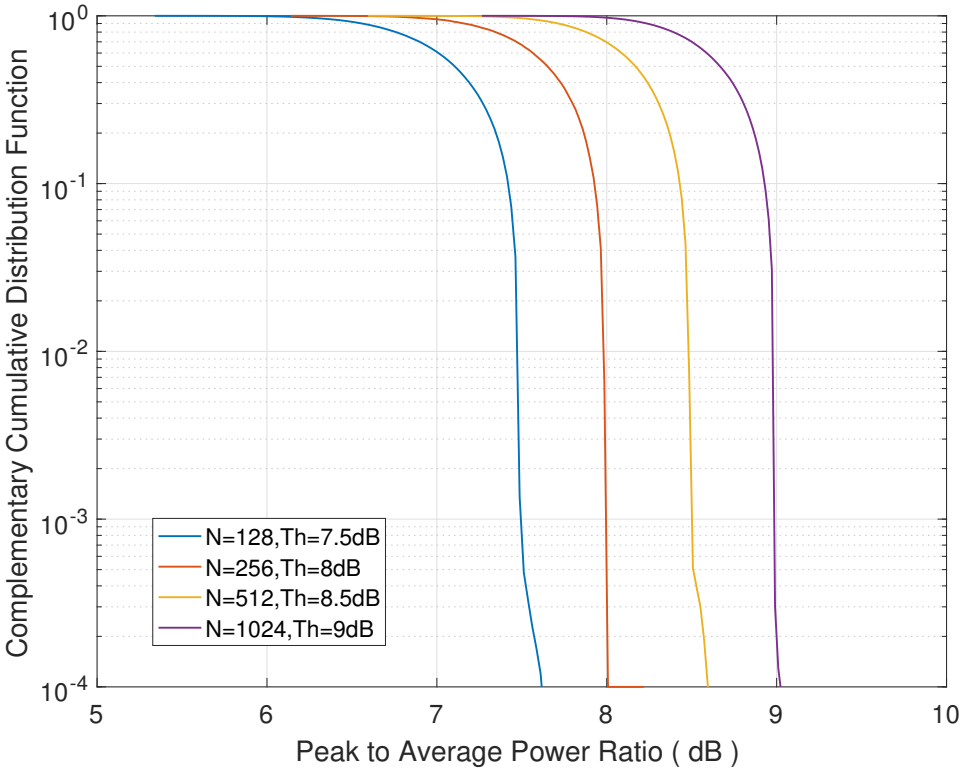

Figure 9: Performance of the system with increasing number of subcarriers N, for threshold Th.

4. PERFORMANCE OF SINGLE CARRIER WAVEFORMS IN MIMO SYSTEMS

In this chapter, performance of single carrier waveforms in MIMO systems are analyzed in terms of BER. The effects of number of users, channel taps, antennas, and channel correlation on the BER performance are investigated. Also performance is investigated in practical channel models for the uplink scenario. In Section 4.1 the uplink channel is considered and in Section 4.2 the downlink channel is considered. In addition, the effect of antenna pre-coding on the PAPR of the signal is investigated for the downlink channel.

4.1. Single carrier - Uplink

The system model of the uplink channel is explained in the first section followed by the simulations. The performance variation with the number of antennas, number of users and with channel state information (CSI) error are studied in the simulations.

4.1.1. System model

A system with K users is considered, each equipped with a single antenna. The base station has M receive antennas. The frequency selective channel has $L+1$ equi-spaced taps, which are Rayleigh distributed. Let $h_k\left[l,m\right]$ be the l^{th} tap in the discrete channel from k^{th} UT to m^{th} receive antenna at the BS. The notation in [28] is followed.

Let $\mathbf{x}[n] = \left(x_1\left[n\right], x_2\left[n\right], ,,,x_K\left[n\right]\right)^T$ be the transmitted signal vector and $\mathbf{w}[n] = \left(w\left[n,1\right], w\left[n,2\right], ,,,w\left[n,M\right]\right)^T$ be the additive noise vector.

The received signal $\mathbf{y}[n] = \left(y\left[n,1\right], y\left[n,2\right], ,,,y\left[n,M\right]\right)^T$ will be

$$y[n] = \sum_{l=0}^{L} \mathbf{H}[l]x[n-l] + \mathbf{w}[n], \tag{7}$$

where, $\mathbf{H}[l]$ =

$$\begin{bmatrix} h_1[l,1] & h_2[l,1] & \dots & h_K[l,1] \\ h_1[l,2] & h_2[l,2] & \dots & h_K[l,2] \\ \vdots & \vdots & \ddots & \vdots \\ h_1[l,M] & h_2[l,M] & \dots & h_K[l,M] \end{bmatrix}.$$

Considering that channels have $L+1$ paths, the transmitted symbol vector at time n is estimated by received vectors up to time slot $n+L$. Therefore, assembling the transmit, receive, and noise vectors as follows;

$$\mathbf{Y} = (\mathbf{y}[n+L], \mathbf{y}[n+L-1], ,,,\mathbf{y}[n])^T, \tag{8}$$

$$\mathbf{X} = (\mathbf{x}[n+L], \mathbf{x}[n+L-1], ,,,\mathbf{x}[n-L])^T, \tag{9}$$

$$\mathbf{W} = (\mathbf{w}[n+L], \mathbf{w}[n+L-1], ,,,\mathbf{w}[n])^T. \tag{10}$$

Then defining channel matrix as

$$\mathbf{H} = \begin{bmatrix} \mathbf{H}[0] & \mathbf{H}[1] & \dots & \mathbf{H}[L] & \dots & & \\ & \mathbf{H}[0] & \mathbf{H}[1] & \dots & \mathbf{H}[L] & \dots & \\ & \ddots & \ddots & \dots & \ddots & & \\ & \dots & & \mathbf{H}[0] & \mathbf{H}[1] & \dots & \mathbf{H}[L] \end{bmatrix}. \tag{11}$$

Thus,

$$Y = \mathbf{HX} + \mathbf{W}. \tag{12}$$

The maximum likelihood (ML) receiver is

$$\mathbf{H^H Y} = \mathbf{H^H HX}. \tag{13}$$

Given that the number of base station antennas, M, is large enough, a simplified receiver is therefore, [23, 28]

$$\tilde{\mathbf{x}}[n] = \frac{1}{M}\mathbf{H^H Y}. \tag{14}$$

Up to now, ideal CSI is assumed to be available at the receiver side. Next, the scenario where there is uncertainty in the CSI is considered. This can be modeled as

$$\tilde{h}[n,m] = h[n,m] + \epsilon[n,m], \tag{15}$$

where, the estimation error or the uncertainty, $\epsilon[n,m]$ is modeled as a circularly symmetric complex Gaussian random variable, and is independent for each tap.

4.1.2. Simulations

Here, the performance of the system is investigated with different parameters in terms of the number of users, antennas, and channel taps. 16QAM is used as the modulation scheme. The Fig. 10 shows the performance with different number of users with ideal CSI, whereas the Fig. 11 shows the performance with different number of antennas. The results indicate that the reduced complexity receiver performs well in the given antenna regime. This is an important observation since it is not optimal. In Fig. 12, single and multiple user performance is considered for higher number of taps with ideal CSI and with errors in CSI ($0\ dB$ error in variance). A higher number of users cause additional interference. The degradation in performance compared to ideal CSI is seen to increase with the number of users. Having a larger number of antennas can address both these issues to a certain extent as seen in the results. Even in the case of OFDM this is the scenario as well, that the performance is compromised with multiple users operating within the same set of subcarriers.

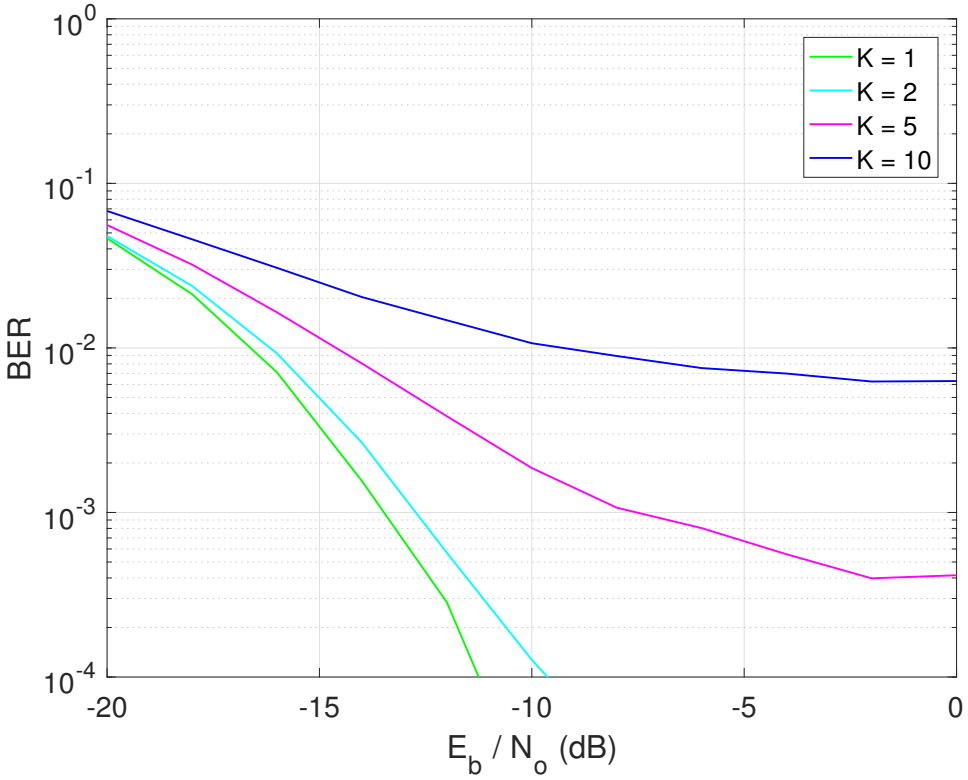

Figure 10: Uplink performance of a system with 300 antennas and 20 channel taps for variable users.

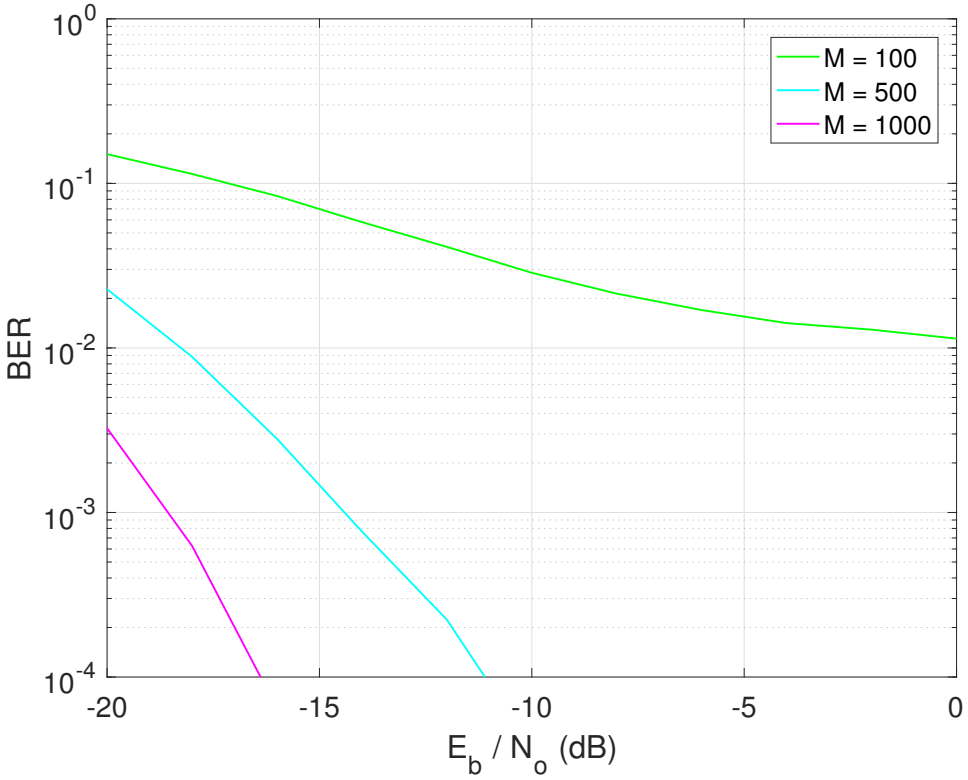

Figure 11: Uplink performance of a system with 4 users, 20 channel taps for variable number of receive antennas.

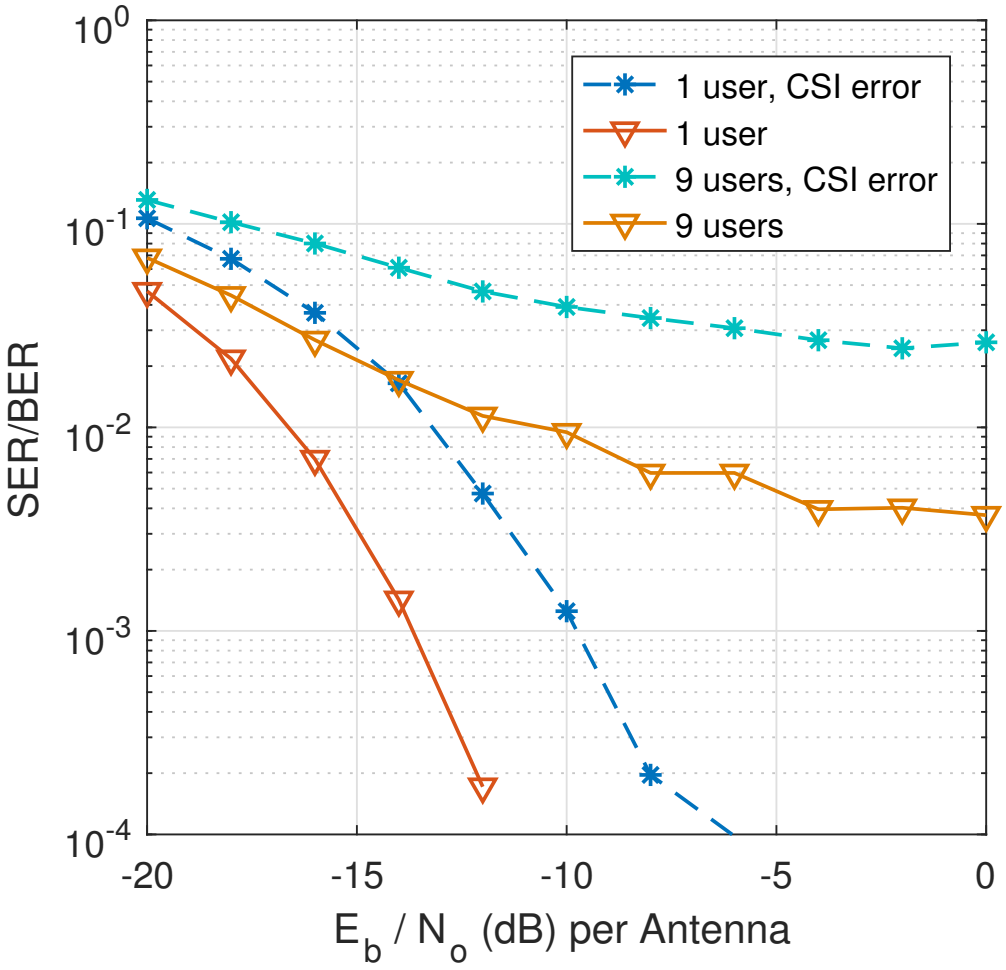

Figure 12: Uplink performance of a system with 300 receive antennas, 9 users and 0 dB error in CSI.

4.2. Single carrier-Downlink

Performance of single carrier-downlink System model of the downlink channel is investigated in this section.The system model is explained in the first subsection followed by the simulations of BER for different number of users, antennas and with CSI error. In the third subsection, the effect of antenna pre-coding on the PAPR of the signal is studied. BER for the different correlated channels are studied in the last sub section.

4.2.1. System model

In the case of downlink a similar scenario with the base station and users is assumed. The main difference in this case is that the transmit signal will be precoded based on the channel response or channel state information at the transmitter (CSIT). Thus following [27] if the information symbol vector is $\mathbf{s}[i] = (s_1[i], s_2[i], ,,,s_K[i])^T$, the transmit vector is given by

$$\mathbf{x}[i] = \sqrt{\frac{\rho_f}{MK}} \sum_{l=0}^{L-1} \mathbf{H}_l \mathbf{D}_l^{1/2} \mathbf{s}[i+l], \tag{16}$$

where, ρ_f is the long term average total power at the BS antennas. The received signal vector at time i is therefore [27],

$$\mathbf{y}[i] = \sum_{l=0}^{L-1} \mathbf{D}_l{}^{1/2} \mathbf{H}_l{}^H \mathbf{x}[i-l] + \mathbf{n}[i]. \tag{17}$$

Here, $\mathbf{D}_l = (d_l[1], d_1[2], ,,,d_l[K])$, where, $d_l[K] \geq 0, l = 0, 1, ,L-1$ gives the power delay profile (PDP) of each user K. Further PDP for each user is normalized such that,

$$\sum_{l=0}^{L-1} d_l[k] = 1, k = 1, ,,,,, K. \tag{18}$$

Due to the orthogonality in the channel matrices [23], as in the case of uplink due to the large number of antennas at the base station side, the information symbol vector can be estimated with asymptotic optimality. The issue of CSIT error which is normally unavoidable in this case in any practical set up is also investigated.

4.2.2. Simulations

Here, the performance of the system is investigated with different parameters in terms of the number of users, antennas, and channel taps. The degradation in performance compared to single tap is not very significant implying that the reduced complexity receiver is performing quite well. Fig. 13 shows the performance with a different number

of antennas under ideal CSI. The performance in the presence of channel uncertainty is investigated in Fig. 14. The degradation in the presence of CSIT error ($0dB$) seems quite significant.

These also show a similar performance to the uplink curves in the sense that there needs to be a larger number of antennas to compensate for interference and non-idealities. As a general conclusion, therefore, one can say that the single carrier system performs satisfactorily in the massive MIMO paradigm expected to be strengthened by the application in the mmWave frequencies.

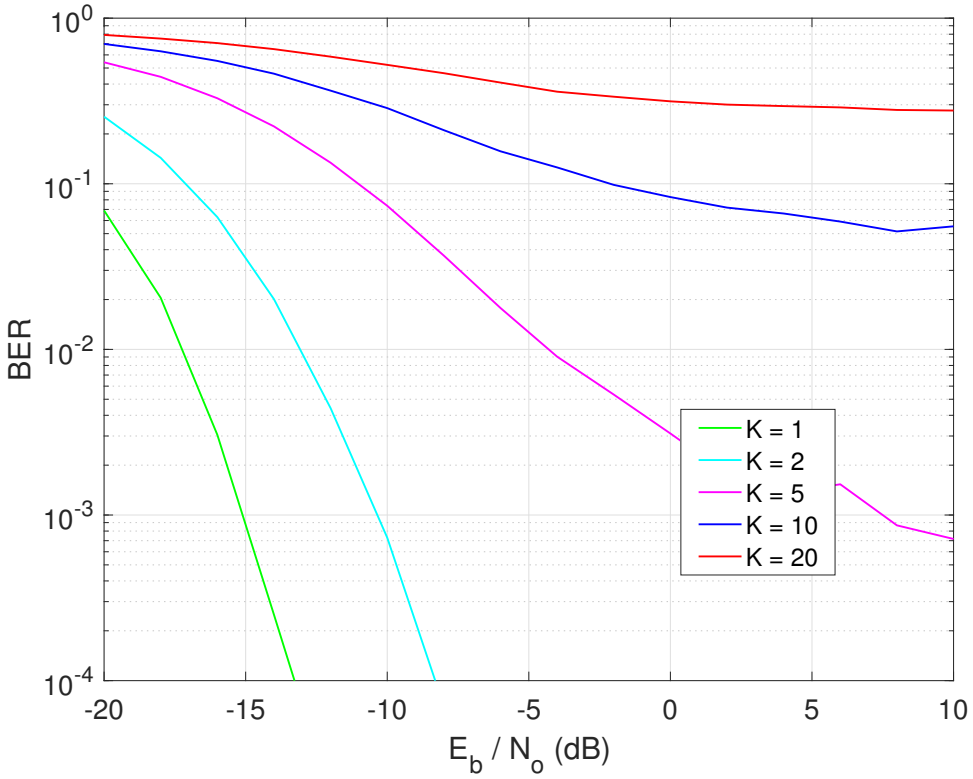

Figure 13: Downlink performance of a system with 500 antennas and 5 channel taps for variable users.

4.2.3. PAPR Analysis

As mentioned previously, to fairly compare an OFDM system with a downlink single-carrier system, the issue of PAPR needs to be considered. This is due to the fact that the channel is frequency selective channel and pre-coding is carried out to match the transmit symbols to the channel, which unlike in the case of flat fading, is a bit more involved due to multiple taps. To better approximate the PAPR of continuous time OFDM signals, OFDM samples are taken by several times oversampling [5, 13], where, a survey of methods dealing with this issue is presented. Following the same arguments and assuming a certain carrier frequency f_c PAPR for single-carrier systems can be calculated.

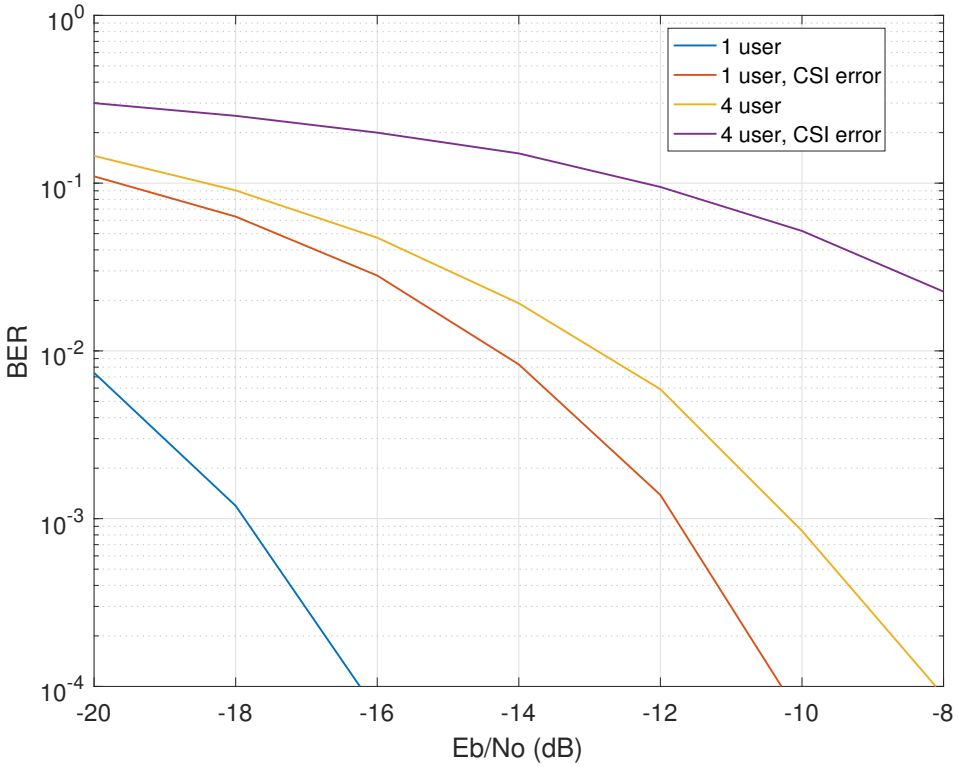

Figure 14: Downlink performance of a system with 300 transmit antennas and 0 dB error in CSI.

Using (16) as the transmit signal, the PAPR is given by

$$PAPR\{x\,[n]\} = \frac{\max_{0\leq n\leq N}\left[|x\,[n]\,|^2\right]}{E\left[|x\,[n]\,|^2\right]}. \tag{19}$$

CCDF for PAPR is the probability of OFDM symbols with PAPR exceeding some threshold λ. In the case of OFDM a typical plot is shown in Fig. 15. The Fig. 16 shows the CCDF plot of single-carrier PAPR. It can be seen that PAPR increases as the number of channel taps increases. As the Fig. 16 shows the PAPR value can change significantly when a pre-coded downlink signal is considered. The values are seen to vary from $6-10\ dB$ without any other modifications such as windowing etc.

In the case of OFDM systems this can be as high as $12\ dB$ as seen in Fig. 15 [5] and normally some methods are employed for the reduction of these values. Similar approaches can also be considered for the single carrier system which can lower the values to $4-8\ dB$ range [19]. One can therefore say there is still a significant PAPR advantage in using single-carrier systems in the downlink coupled with the reduced complexity receiver.

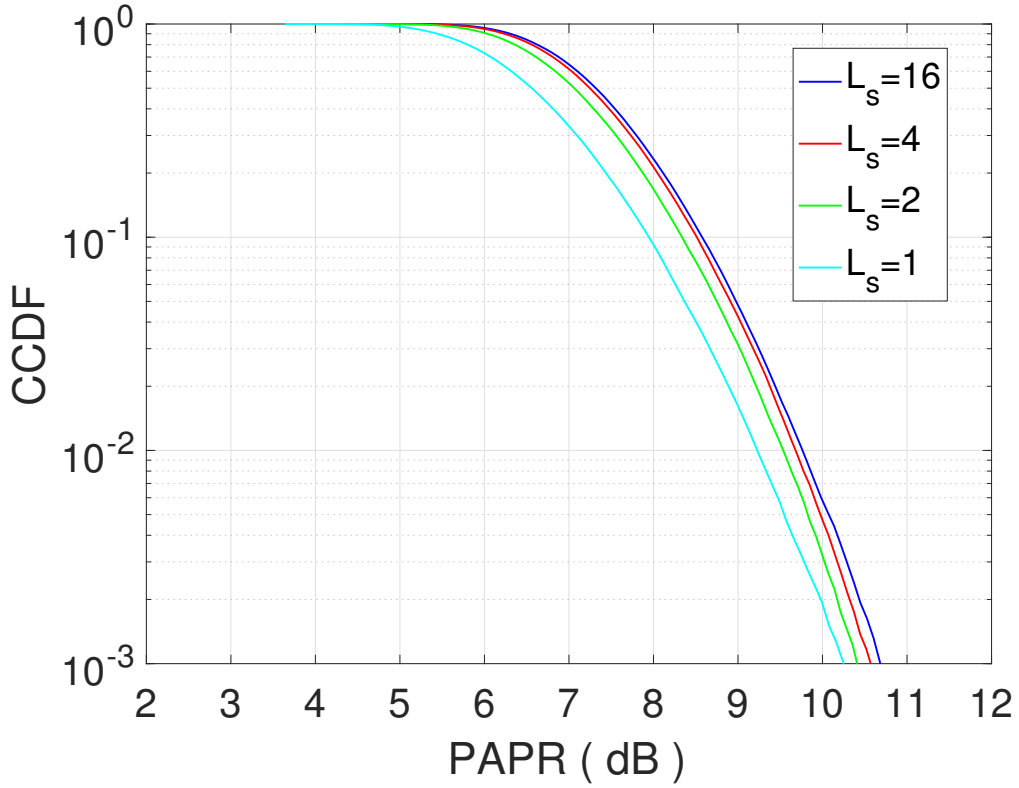

Figure 15: PAPR performance of OFDM for variable oversample factor L_s.

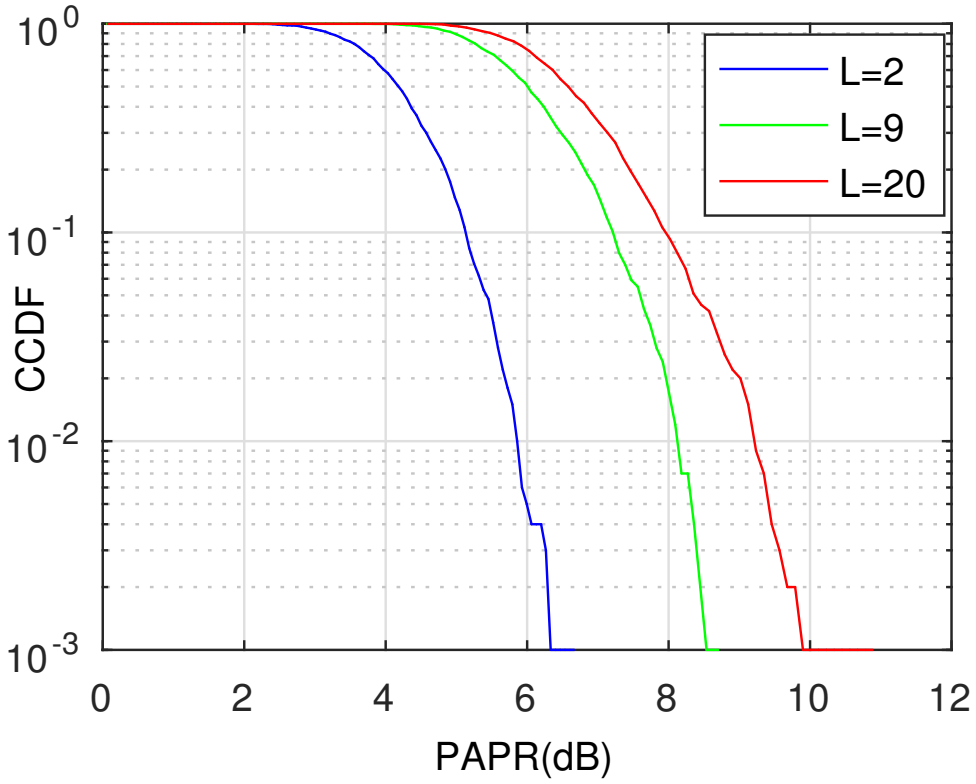

Figure 16: PAPR performance with variable channel taps L.

4.2.4. Correlated Channels

In the previous cases, another effect which is normally present in multiple antenna systems were not considered. This is the correlation among antennas which also is a significant factor as the number of antennas increases. Therefore, several cases with two of the possibilities; exponential and uniform linear array (ULA) correlation were considered in the following sections.

Exponential correlation

Let $\mathbf{a}$ be the exponential correlation (Exp) coefficient. Then exponential correlation matrix of a channel with M BS antennas will be

$$\mathbf{t} = \begin{bmatrix} 1 & a & \dots & a^{M-1} \\ a & 1 & \dots & a^{M-2} \\ & \ddots & \ddots & \vdots \\ a^{M-1} & & \dots & 1 \end{bmatrix}. \tag{20}$$

Uniform linear array

In a typical ULA, where, antennas are placed long a line with length D, the distance between m^{th} and m_0^{th} antennas will be [29]

$$d = \frac{(m - m_0)D}{M - 1}. \tag{21}$$

Then, the spatial correlation between any two antennas with distance d will be

$$\rho(\frac{d}{\lambda}) = \frac{J_0(2\pi d)}{\lambda}. \tag{22}$$

where, $J_0(.)$ is the zeroth order Bessel function of the first kind.

Simulations

Figs. 17 and 18 show the BER curves for different correlated channels with quadrature phase shift keying (QPSK) and 8 phase shift keying (8PSK) respectively with clear degradation for higher correlation. The correlation is unavoidable given the cases where the close spacing of antennas is likely or needed even in the mmwave region. The application of suitable channel codes may be one way to address this [36, 37].

4.3. Practical Channel Models

It is also important to evaluate the performance of a single carrier system with a measured channel model, in this case at $10\ GHz$ as well to get a more realistic idea about the performance. Here a Quadriga based model modified as given in [24, 25] is employed. The coefficients of the channel matrix are in the order of $10^{-5} - 10^{-9}$ which

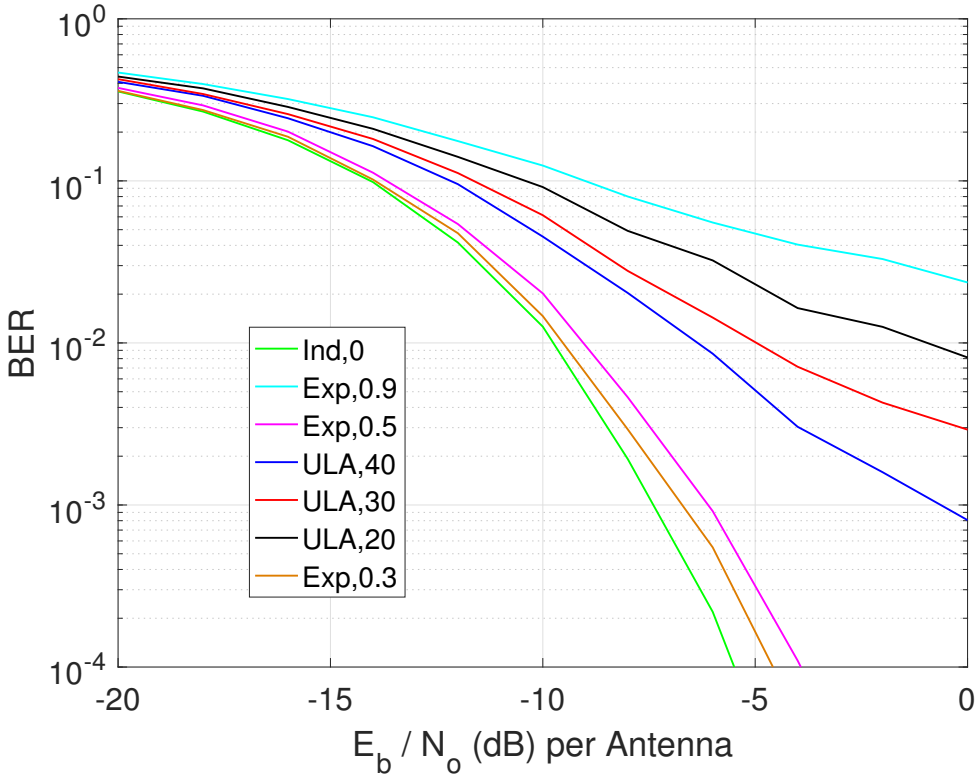

Figure 17: Downlink QPSK performance of a system with 200 transmit antennas, 5 channel taps, and 4 users for correlated channels.

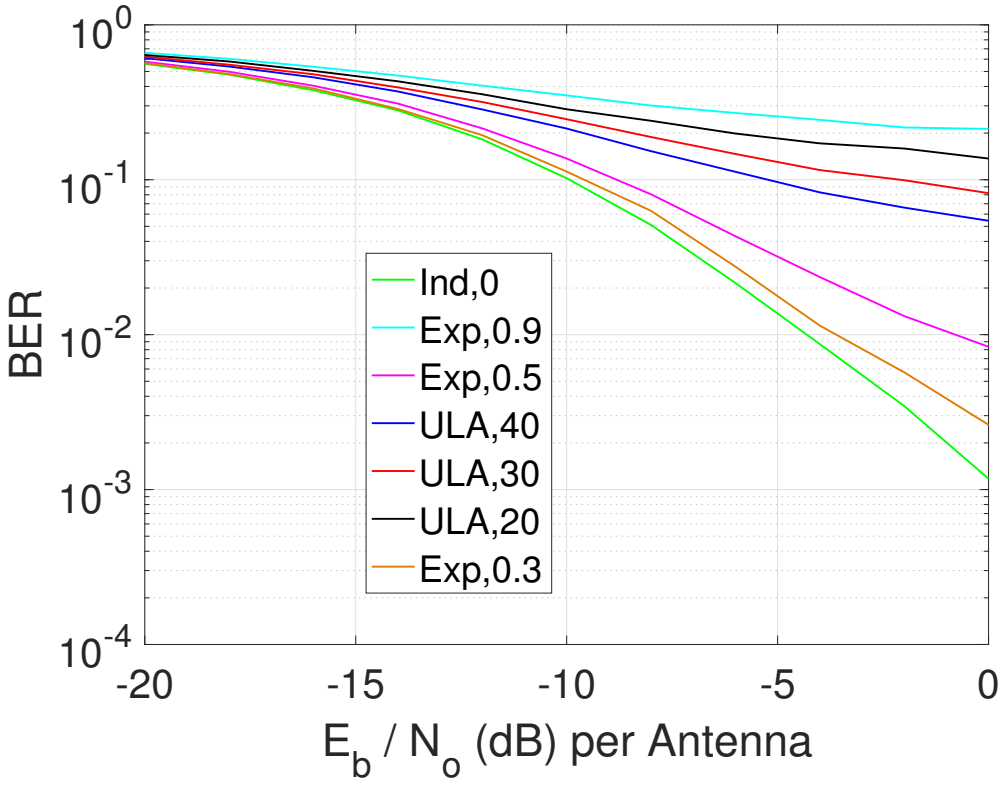

Figure 18: Downlink 8PSK performance of a system with 200 transmit antennas, 5 channel taps, and 4 users for correlated channels.

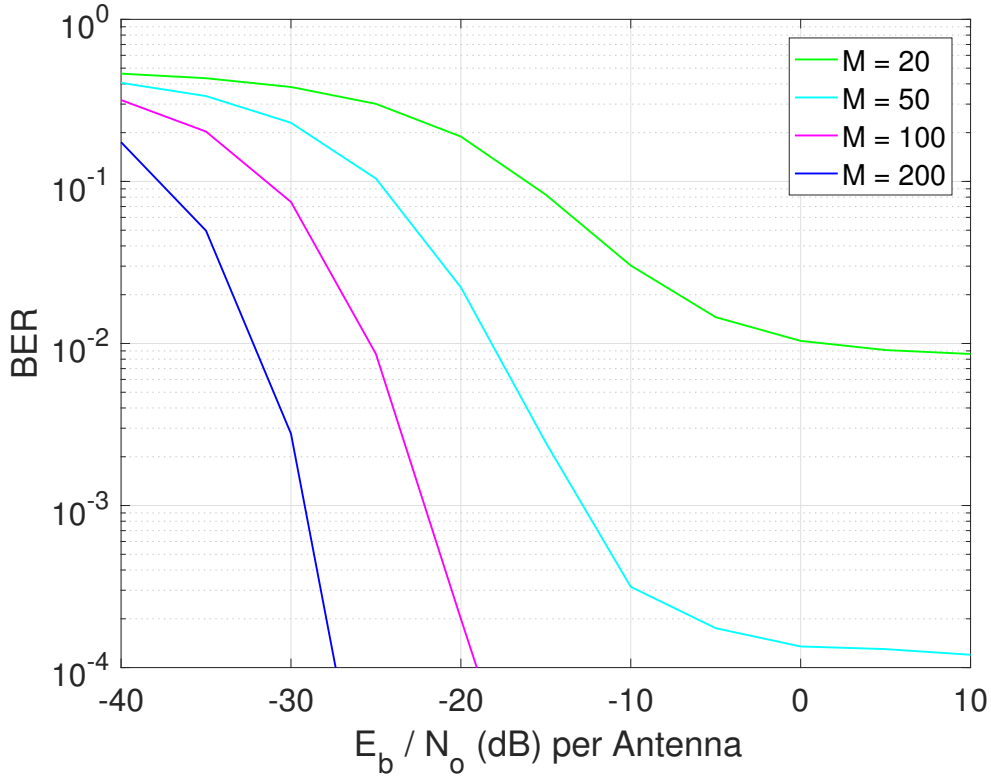

Figure 19: Uplink QPSK performance for a system with 9 channel taps, 4 users and variable number of receive antennas in a practical channel model.

is very low. Thus in our case the channel matrix is normalized across M BS antennas to produce coefficients in the order of 10^{-1}.

4.3.1. Simulations: Uplink

Figs. 19 and 20 show the BER curves for QPSK and 8PSK modulated signals in practical channel models. QPSK modulated signals have acceptable performance with 50 BS antennas for four user case. In the case of 8PSK with 100 BS antennas, a higher number of users will degrade the performance.

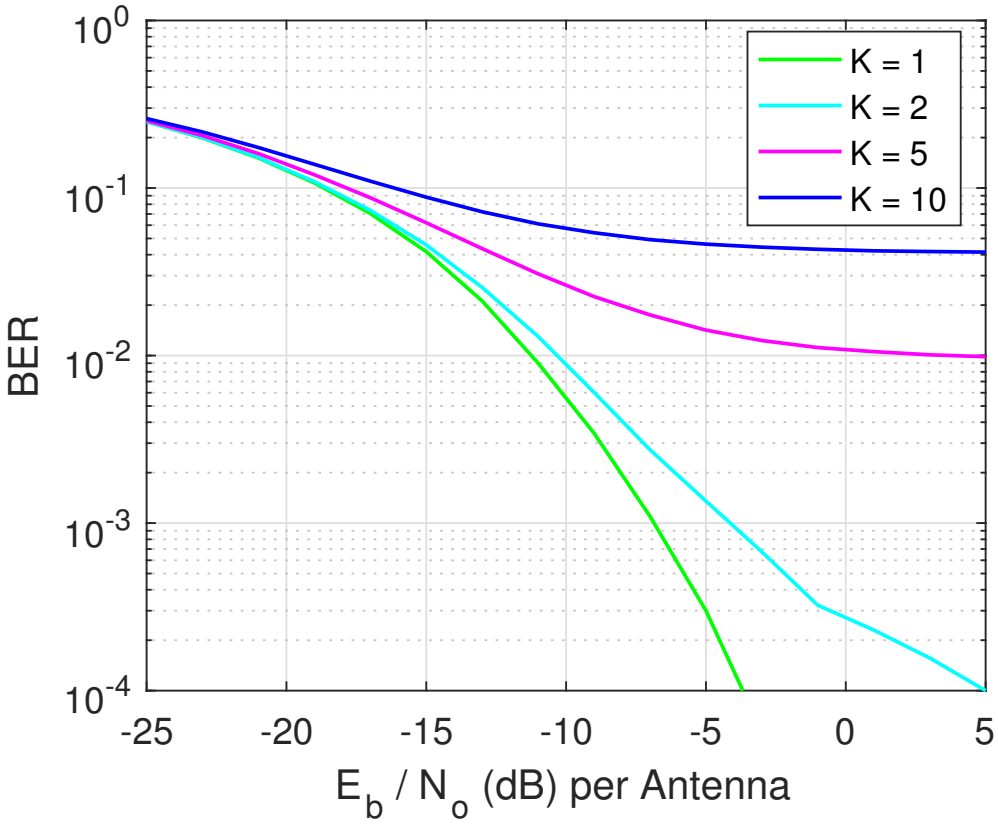

Figure 20: Uplink performance of an 8PSK system with 200 receive antennas and variable users in a practical channel model.

5. CHANNEL CODING

Candidate coding schemes for the eMBB scenario of 5G NR are evaluated in this chapter. In the first section, some performance aspects of the candidate coding schemes are discussed along with the decoding algorithms. In the second section, simulation parameters are stated, followed by the simulation results in the third section.

5.1. Candidate Coding Schemes

5.1.1. Turbo codes

The 3GPP LTE standard specification parameters [38] are used for the simulations [41] and the discussions of turbo codes in this thesis. Each convolutional turbo code encoder outputs two streams, one systematic stream and one parity stream. Input information bits to the second encoder is fed after interleaving the input bit stream.

For iterative decoding of the parallel concatenated encoding scheme, the turbo decoder uses a MAX-Log-MAP algorithm as the constituent decoder component. The internal interleaver of the decoder is identical to the one the encoder uses.

Since there are three output streams; a systematic bit stream and two parity streams in the encoder, coding rate for this LTE system is 1/3. Other higher rates are achieved through puncturing of some parity bits. Assume R and N_b are code rate and coded block length respectively, for all the coding schemes. Assuming the decoder has a memory length of M_b bits for the component code and I number of iterations, turbo codes has $16 \cdot I \cdot R \cdot N_b \cdot 2^{M_b}$ additions and $8 \cdot I \cdot R \cdot N_b \cdot 2^{M_b}$ logical operations. [36]

For comparison, computational complexity of each coding scheme is expressed in terms of equivalent additions. Number of equivalent additions for different operations are stated in Table 4 [36].

5.1.2. LDPC codes

Quasi-Cyclic LDPC (QC-LDPC) codes are used for simulations and discussions throughout this thesis. A QC-LDPC matrix is characterized by the parity check matrix H. It consists of small square blocks which are the zero matrix or circulant permutation matrices. An advantage of QC-LDPC code is that it supports variable code lengths which can be easily obtained by adjusting the circulant permutation matrices in H. Sum product algorithm (SPA) is the optimal decoder for LDPC, and min-sum algorithm is a sub optimal algorithm with reduced computational complexity.

While QC-LDPC codes allows reasonable flexibility in code length, puncturing is used to achieve rate-adaptive codes. Assuming d_v and d_c as the average variable and check degrees of the LDPC parity check matrix respectively and P_b as the number of parity bits, min-sum LDPC decoder has $I \cdot (2N_b \cdot d_v + 2P_b)$ additions and $I \cdot (2d_c - 1) \cdot P_b$ max processes [36]. Offset min-sum (OMS) decoder is a reduced complexity version of min-sum decoder where algorithm converges in a smaller number of iterations and it is used as the decoder for the simulations in this thesis.

Table 4: Number of equivalent additions per operation.

Operation	Number of Equivalent additions per operation
Addition, Subtraction	1
Multiplication, Division	1
Comparison	2
Maximum, Minimum	1
Parallel list	1

5.1.3. Polar codes

Polar code construction can be done recursively via Kronecker products and have an encoding complexity of $O(n \log n)$. Complexity of decoding is also the same via successive cancellation (SC) decoding. However, the SC decoder itself is not sufficient to achieve competitive performance as other coding schemes. Hence list decoding is incorporated into SC decoder which results in the SC list (SCL) decoder [39]. In addition a cyclic redundancy check bits (CRC) are used to further enhance the code performance at an expense of increased complexity.

Construction of the polar codes requires knowledge about specific channel conditions, hence not versatile. While different code rates can be achieved by changing the number of frozen bits in polar codes, a puncturing scheme is needed to obtain some code lengths. SC decoder has a complexity of only $N_b \cdot Log_2 N_b$ additions where as SCL decoder with list size of L_p has a complexity of $L_p \cdot N_b \cdot log_2 N_b + (N_b - P_b) \cdot L_p \cdot Log_2 L_p$ additions [36].

5.2. Simulations

The candidate coding schemes are simulated with QAM and AWGN channel in the first set of simulations. Rayleigh fading channel with AWGN is considered with CSI available in the second set of simulations.

Coding parameters are given in Table 5 and performance is evaluated in terms of BLER and BER. For turbo codes LTE-Advanced encoder with two 8-state constituent encoders and a block interleaver is used. At the receiver, the scaled MAX-Log-MAP decoder with scaling factor of 7, and iteration count of 8 is used. The code rate of original turbo code is 1/3 and higher rate codes are obtained through puncturing.

In LDPC code simulations, parity check matrices specified in IEEE 802.11n are used for encoding. The OMS decoder with 0.3 as the offset value and 50 iterations is used at the receiver. Different code lengths are obtained by changing the size of base matrix of the parity check matrix.

Polar codes construction is based on construction for AWGN channel as suggested in [40]. The performance is simulated using both SC decoder and CRC aided-SCL

Table 5: Parameters for simulations.

Parameters	Turbo	LDPC	Polar
Channel	AWGN, Rayleigh Fading		
Modulation	QPSK		
Code lengths	128, 512, 1024, 2048, 4096		
Code rates	1/3 , 1/2 , 2/3		
CRC	NA	NA	8
Decoder	max-log-MAP	Offset-min-sum	SC, CRCA-SCL, L=8

decoder (CRCA-SCL) with list size of 8 and 8 CRC check bits for all the code rates and lengths.

Algorithmic complexity of the decoders used for each coding scheme is obtained for block lengths 128 and 4096 in Table 6. This also shows the percentage of complexity with respect to turbo code in the percentage column.

5.3. Simulation results in AWGN channel

In Fig. 21 to 24, BLER and BER of the coding schemes are plotted against the energy per bit to noise power spectral density ratio (E_b/N_0) for Turbo, LDPC and Polar codes for different block lengths and coding schemes.

In summary, at the block-length of 128 bits (Fig. 21), polar codes with CRCA-SCL decoder outperforms turbo and LDPC codes for all the 3 rates. As the block length increases LDPC and Turbo performance comes close to polar codes with CRCA-SCL decoder performance. For example, at the block length of 512 bits (Fig. 22) , polar codes with CRCA-SCL decoder has similar performance as Turbo for rate 1/3 in BLER. But turbo outperforms polar codes in BER at this block length and rate.

When the block length increases as in Fig. 23, turbo codes outperform polar codes with CRCASCL decoder and LDPC for rate 1/3. For rates 1/2 and 2/3 LDPC has better performance than polar or turbo. It should be noted that LDPC codes performs relatively well even without the use of CRC bits, hence this performance can be further enhanced by adding CRC at cost of increased complexity.

In terms of algorithmic complexity as computed in the Table 6, turbo and LDPC codes shows similar complexity in rate 1/3. But for all the other rates turbo codes has relatively higher complexity. SC decoder of Polar codes has the lowest complexity for all rates and SCL decoder with list size of 8 has about 10 times the complexity of SC

Table 6: Decoding complexity of coding schemes.

Block length	Coding Scheme	Complexity ($\times 10^3$)			Percentage		
		1/3	1/2	2/3	1/3	1/2	2/3
128	Turbo	65.5	98.3	131.1	100%	100%	100%
	LDPC	66.0	57.2	48.5	100.7%	58%	37%
	Polar SC	1.0	1.0	1.0	1.5%	1.0%	0.8%
	Polar SCL	11.0	11.0	11.0	16.8%	11.2%	8.4%
4096	Turbo	2097.1	3145.7	4194.3	100%	100%	100%
	LDPC	2112.0	1831.9	1551.9	100.7%	58.2%	37.0%
	Polar SC	53.2	53.2	53.2	2.5%	1.7%	1.3%
	Polar SCL	524.0	524.0	524.0	25.0 %	16.7%	12.5%

decoder. It should be noted that these complexities are based on the assumptions in the Table 6 and actual implementation complexity may differ in practical scenarios.

5.4. Coding performance in fading channel

5.4.1. System model

An uncorrelated fading channel with AWGN is used as the channel. Fading gain h is distributed as Rayleigh fading and CSI is assumed to be available at the receiver. Quadrature amplitude modulation (QAM) is the modulation scheme used at the transmitter. Since polar codes are channel dependent, code design for the fading channel is in [42] Soft decision decoding is used in decoders of all three coding schemes using LLR.

LLR calculation for fading channel is as follows. If M is the modulation alphabet size, then the symbol length S is $N/log_2(M)$. y_s and x_s are assumed to be s^{th} received and transmitted symbols respectively, and h_s is assumed to be the complex scaling factor for s^{th} symbol corresponding to Rayleigh channel, and n_s as the AWGN channel with $n_s \sim N(0, \sigma^2)$. Then received signal y_s can be written as

$$y_s = h_s x_s + n_s. \tag{23}$$

If energy of QAM modulated symbol is$\sqrt{E_c}$, then the LLR of the received symbols in AWGN channel can be computed as [43]

$$LLR_{2s-1}^{awgn} = \frac{2\sqrt{E_c}}{\sigma^2}, real(y_s), \tag{24}$$

$$LLR_{2s}^{awgn} = \frac{2\sqrt{E_c}}{\sigma^2}, imag(y_s). \tag{25}$$

For the fading channels, fading coefficient is incorporated into the LLR as [44]

$$LLR_{2s-1}^{fading} = \frac{2\sqrt{E_c}}{\sigma^2}, real(h_s y_s), \tag{26}$$

$$LLR_{2s}^{fading} = \frac{2\sqrt{E_c}}{\sigma^2}, imag(h_s y_s). \tag{27}$$

5.4.2. Simulations

The results are presented from Fig. 25 to Fig. 30. In each plot BLER or BER is shown against the energy per bit to noise power spectral density ratio (E_b/N_0). Fig. 25 to Fig. 27 present BER and BLER performances of the three coding schemes in Rayleigh fading channel for block lengths of 128, 512 and 1024 bits. Fig. 28 to Fig. 30 illustrate AWGN and fading channel performance of turbo, LDPC and polar codes, respectively.

The results indicate that polar codes perform better for lower block lengths compared to the other two coding schemes, especially at lower code rates as in Fig. 25. As the block lengths increase from Fig. 26 to Fig. 27, LDPC and turbo coding show better performances compared to polar coding. At short block lengths, Turbo and LDPC codes have almost similar performances. LDPC shows better performance than turbo codes at longer block lengths for both BLER and BER, especially in higher code rates such as 2/3, LDPC codes exhibit better performance compared to other two schemes.

It is important to note that a similar trend was observed in AWGN channels with these three coding schemes [37]. This fact can be useful for obtaining an estimate for the performance of a coding scheme in a fading channel given the performance of it in AWGN channel or vise versa. Furthermore it can be seen from Fig. 28 to Fig. 30 that all three coding schemes have similar performance difference from AWGN to Rayleigh fading channels.

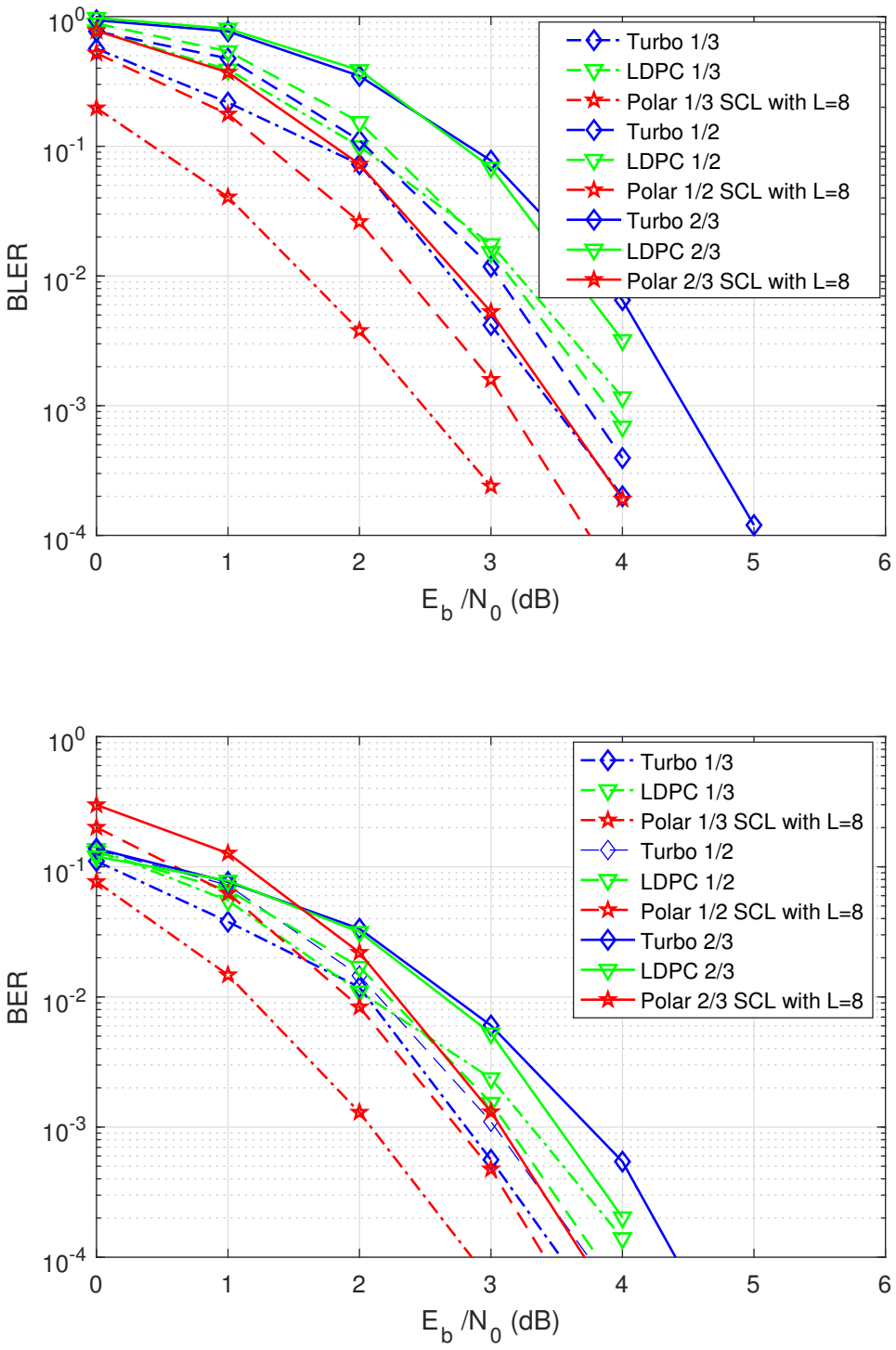

Figure 21: BLER and BER performance of coding schemes at a coded block length of 128 bits and QAM modulation for different code rates.

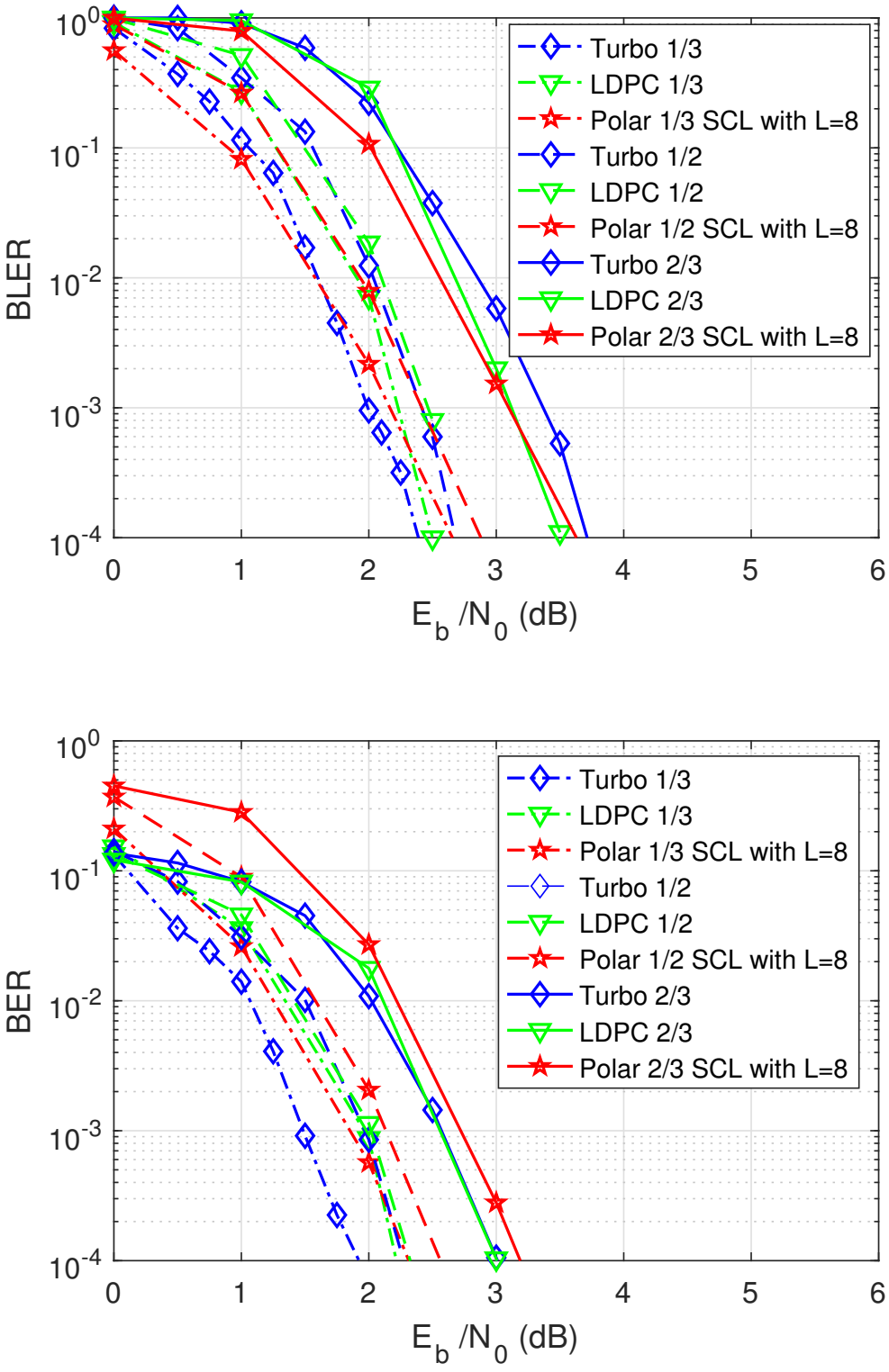

Figure 22: BLER and BER performance of coding schemes at a coded block length of 512 bits and QAM modulation for different code rates.

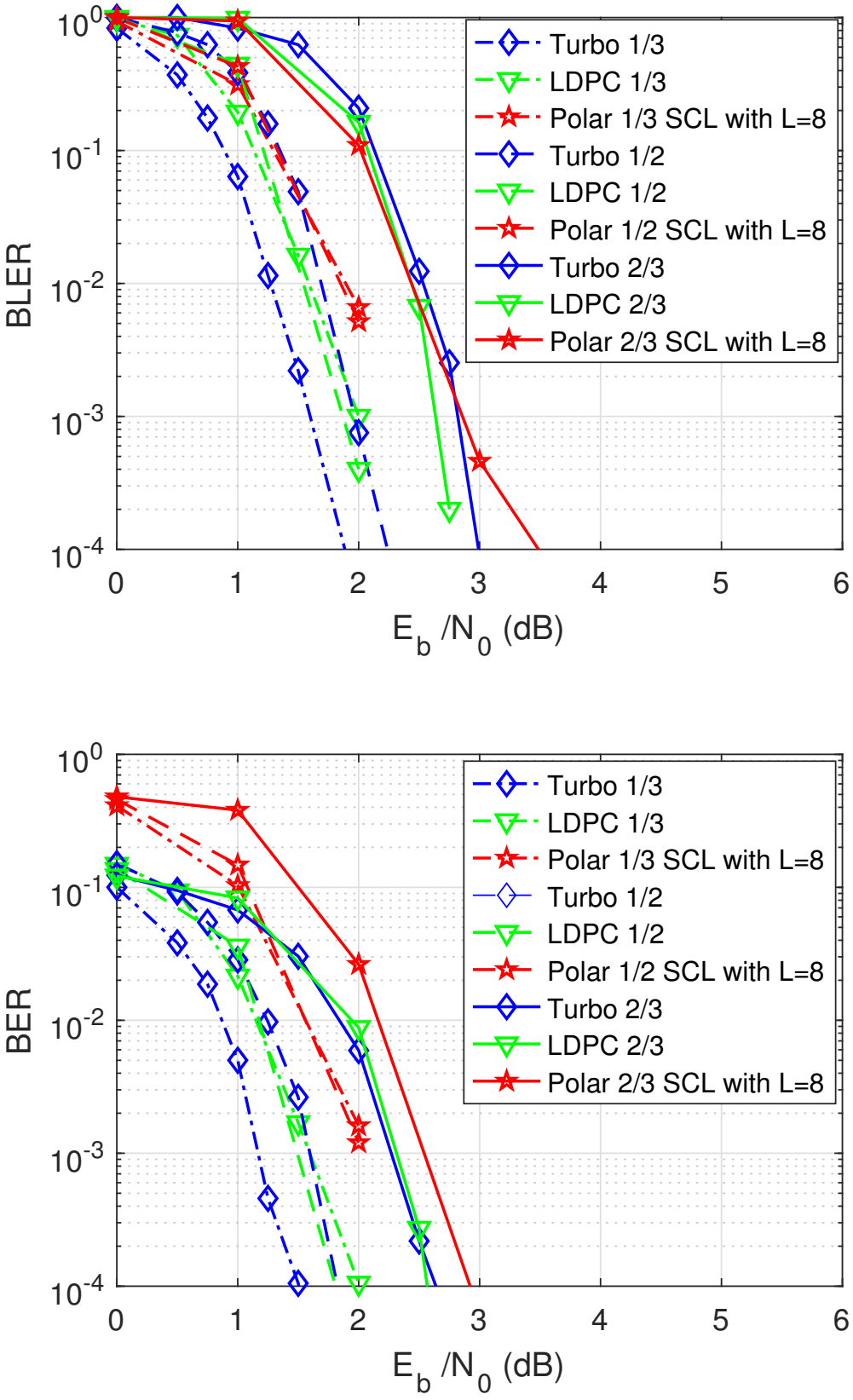

Figure 23: BLER and BER performance of coding schemes at a coded block length of 1024 bits and QAM modulation for different code rates.

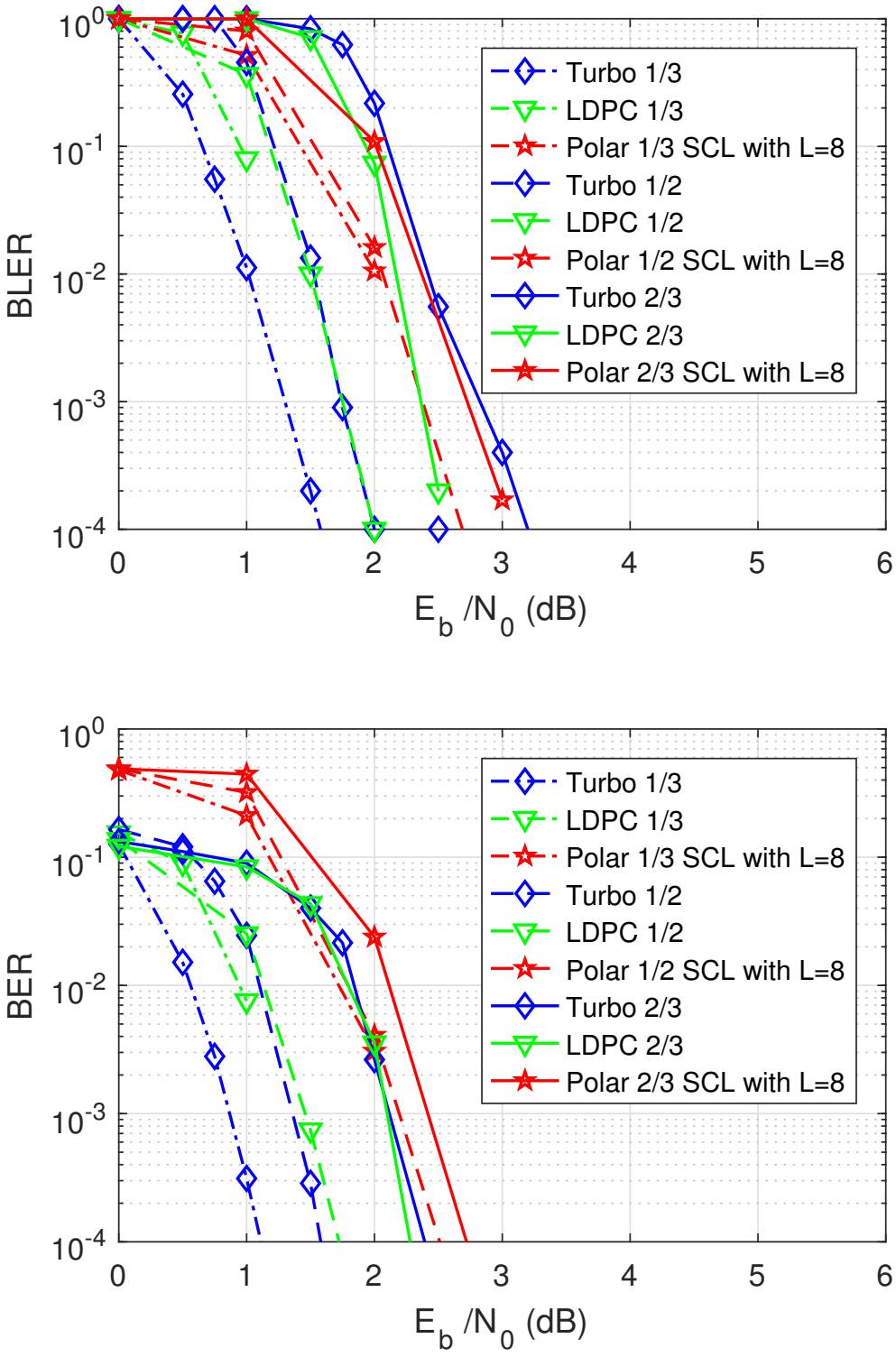

Figure 24: BLER and BER performance of coding schemes at a coded block length of 2048 bits and QAM modulation for different code rates.

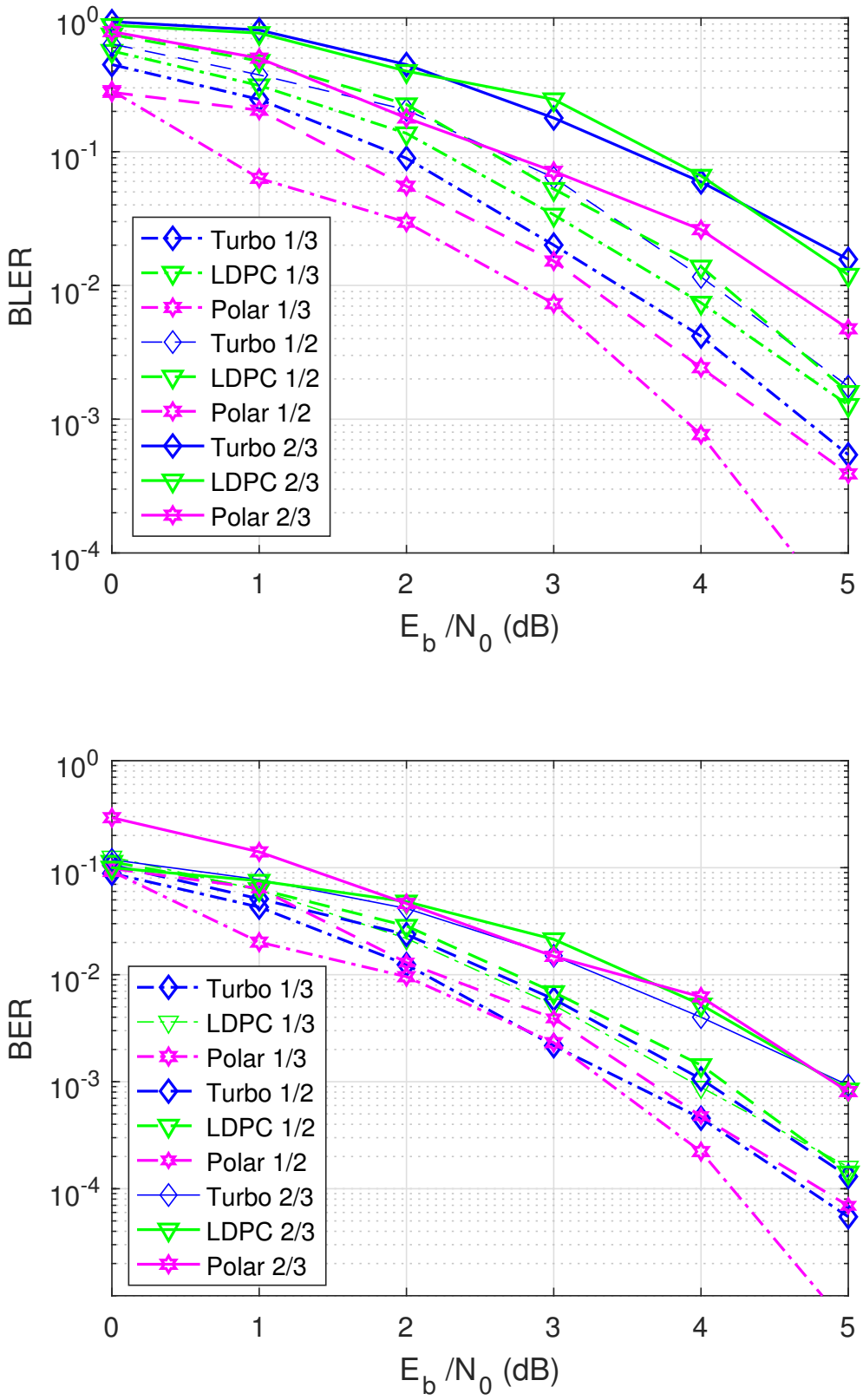

Figure 25: BLER and BER performance of coding schemes at a coded block length of 128 bits and QAM modulation for code rates 1/3, 1/2 and 2/3.

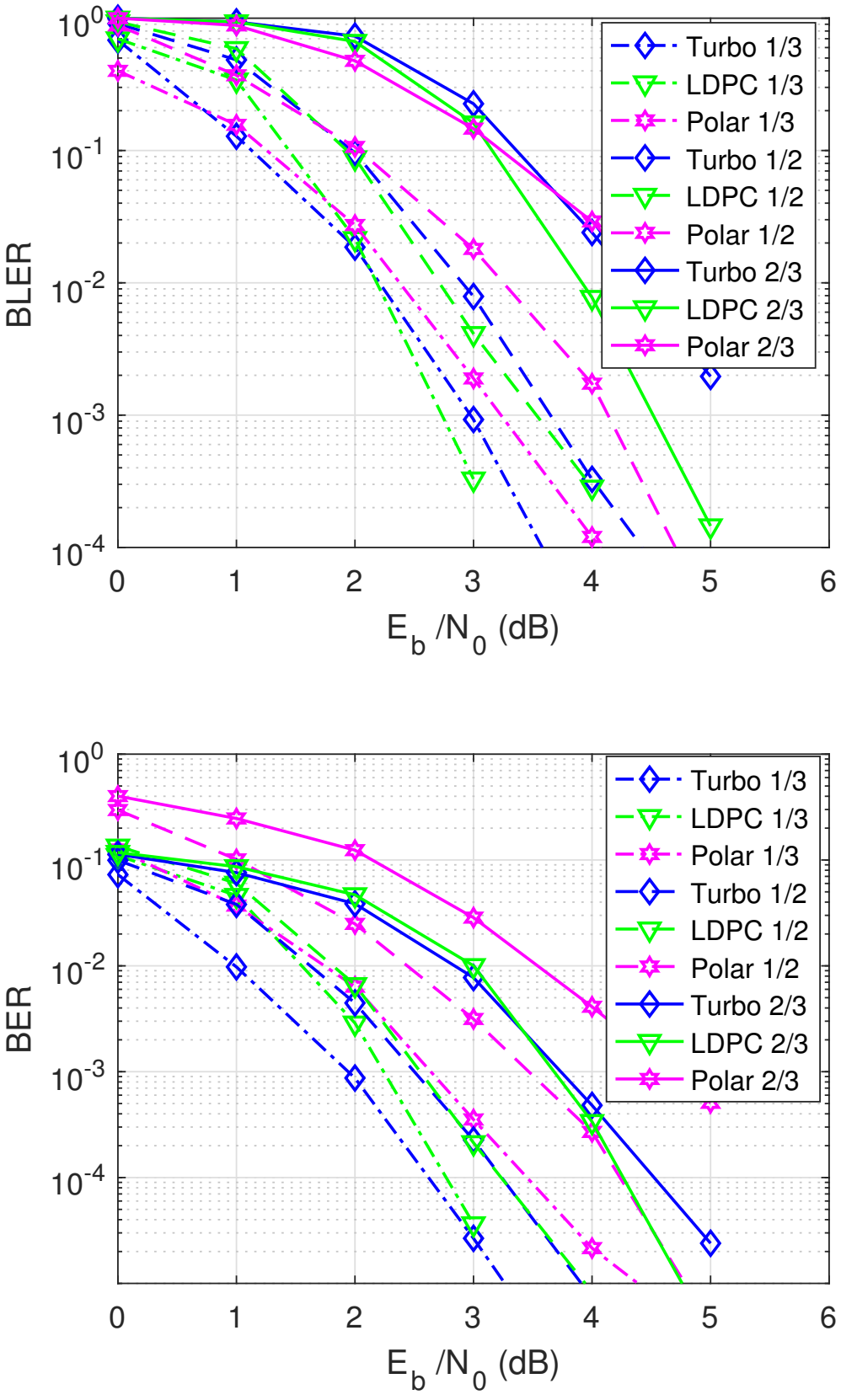

Figure 26: BLER and BER performance of coding schemes at a coded block length of 512 bits and QAM modulation for code rates 1/3, 1/2 and 2/3.

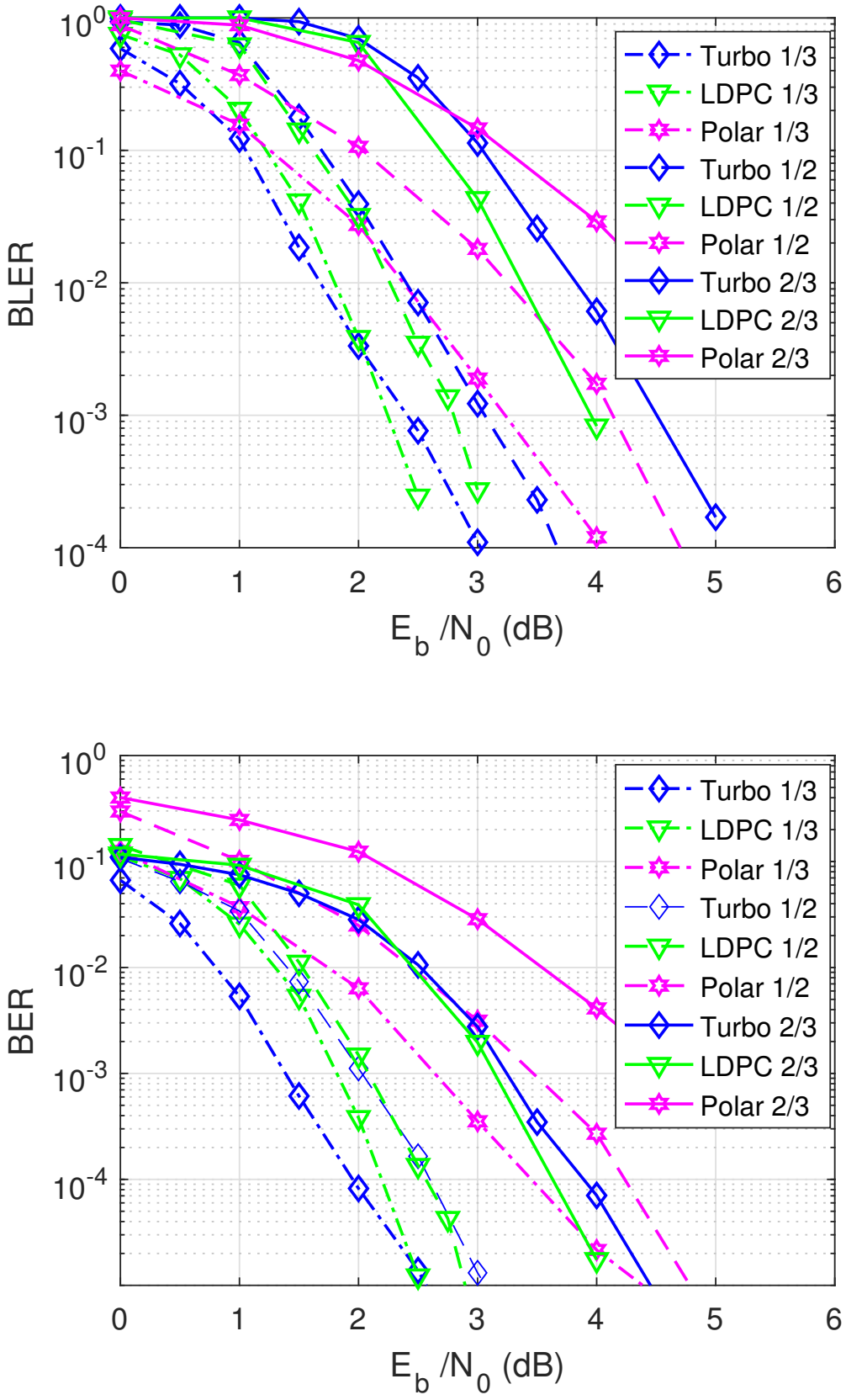

Figure 27: BLER and BER performance of coding schemes at a coded block length of 1024 bits and QAM modulation for code rates 1/3, 1/2 and 2/3.

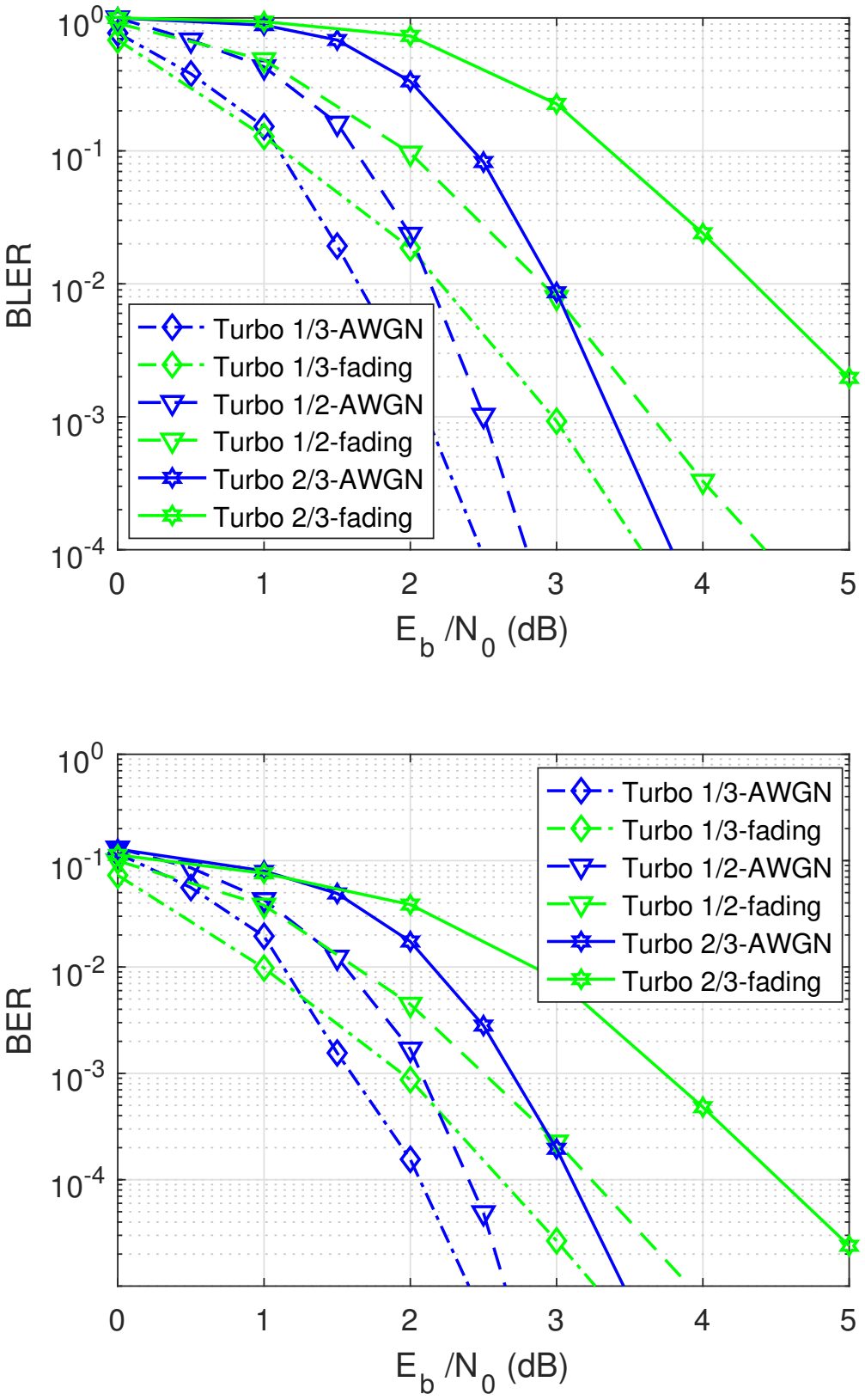

Figure 28: BLER and BER performance of Turbo coding in AWGN and fading channels at a coded block length of 512 bits and QAM modulation for code rates 1/3, 1/2 and 2/3

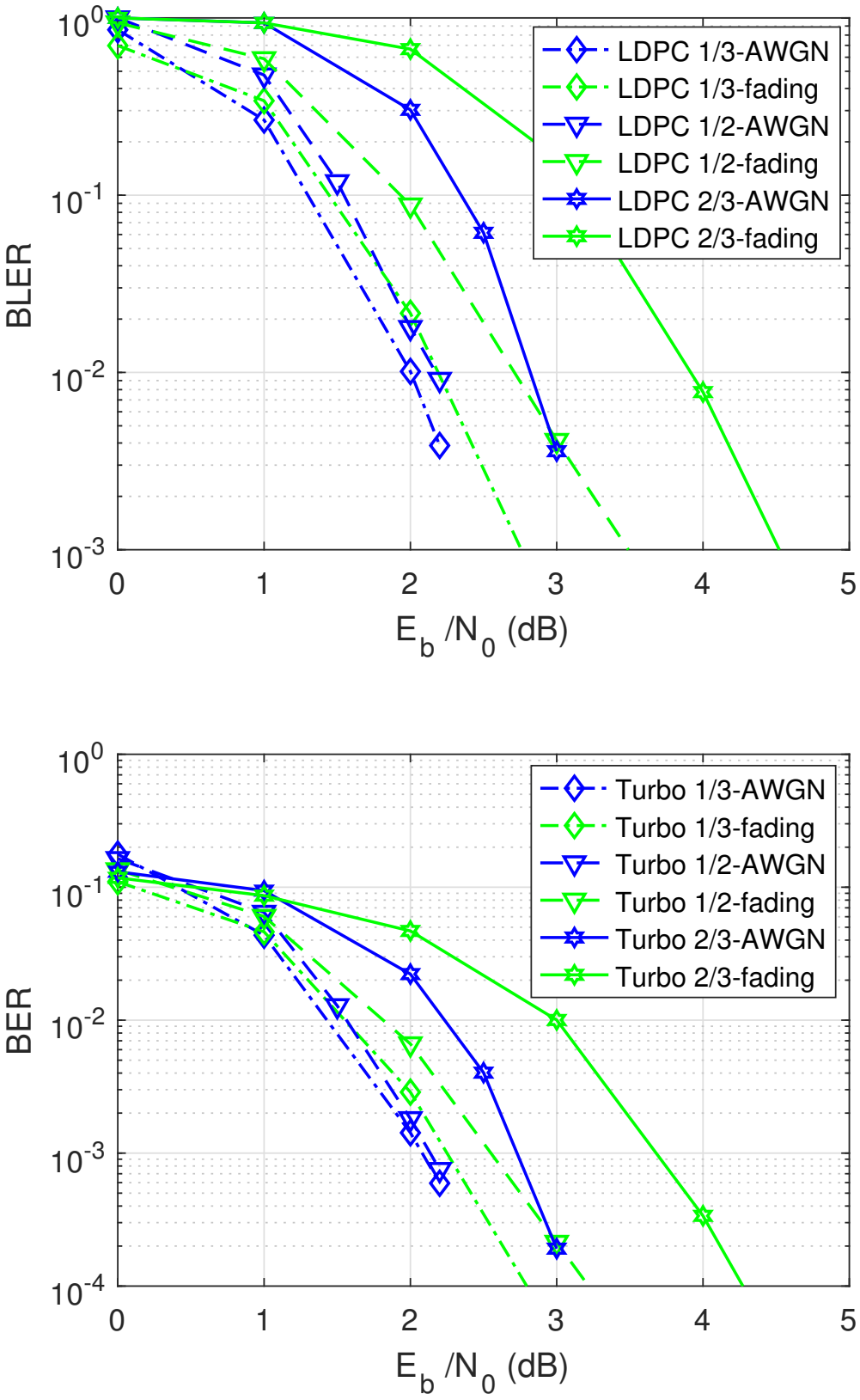

Figure 29: BLER and BER performance of LDPC coding in AWGN and fading channels at a coded block length of 512 bits and QAM modulation for code rates 1/3, 1/2 and 2/3

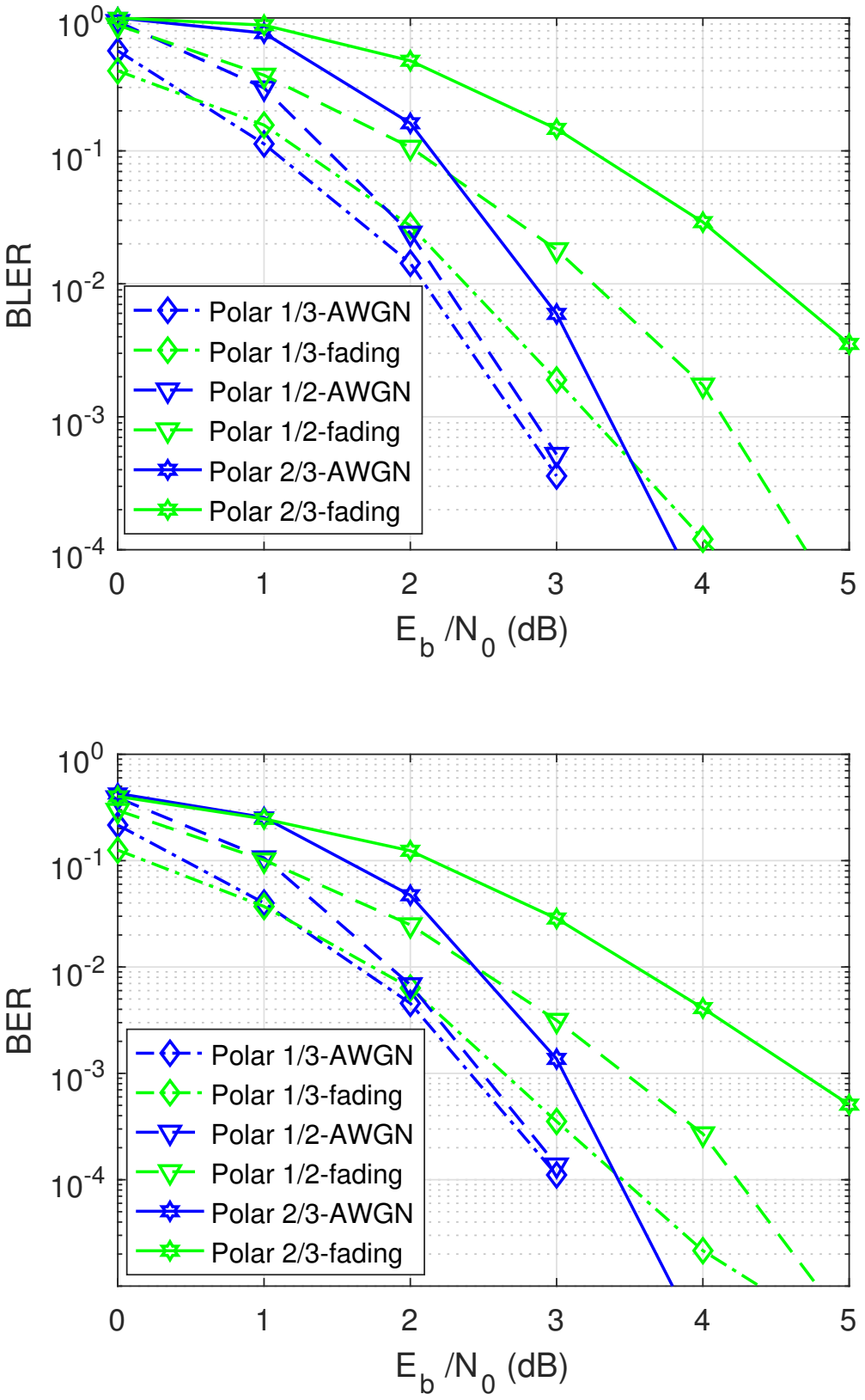

Figure 30: BLER and BER performance of Polar coding in AWGN and fading channels at a coded block length of 512 bits and QAM modulation for code rates 1/3, 1/2 and 2/3

6. CONCLUSION

New air-interface technologies, waveforms and coding schemes for the 5G NR are discussed in this thesis. First, a novel algorithm is proposed to reduce PAPR problem of OFDM waveforms to be considered in 5G RAT. The proposed selective mapping technique uses an array of scramblers and it is evaluated through simulations. It selects the input symbol sequences which result in a PAPR greater than a threshold value and changes those by sending them through scramblers until PAPR gets under the threshold. Search for a low PAPR sequence will be terminated when a sequence is generated with PAPR lower than the preset threshold. Hence computational complexity of this method is significantly decreased from the conventional SLM method. It can be seen from the simulation results that the proposed technique is effective in reducing PAPR from more than 4 dB of the original signal for an arbitrary number of subcarriers. Also we can find a compromise between PAPR reduction and computational complexity by selecting an appropriate threshold value and the overhead of scrambler index side information can be used for trade off in PAPR reduction capability by choosing the size of the scrambler array to a suitable value.

Next we analyzed performance of Single carrier waveforms in MIMO systems as an alternative to OFDM. Performance of a single carrier massive MIMO system is presented for both uplink and downlink with single user and multiple user cases. A variety of channel configurations were investigated, from errors in channel estimate, correlated to measured channels. As opposed to traditional single carrier systems we did not consider any cyclic prefix or frequency domain equalization. A simplified receiver structure is used. It is shown to be effective as the number of antennas increases. The degradation in performance is evident with the number of users. However, this will be the same for any other multi-user system as well. The PAPR performance shows that higher values are obtained with a higher number of taps in the case of the downlink due to beamforming needed. On the other hand in the case of uplink the main processing will be done in the base station. Therefore the proposed single carrier system is a good match there. In general as an access method for mmWave region for new radio in 5G, this is seen to be a viable alternative to multicarrier techniques currently being standardized for the lower frequency range.

Finally we investigated several performance aspects of candidate coding schemes for 5G NR. Performance is analyzed in terms of BER and BLER in both AWGN and fading channels. For block lengths around 100 bits, turbo codes have better performance than polar and LDPC codes. However, LDPC codes exhibit relatively good performance in all the coding rates and block lengths. Furthermore we should note that LDPC codes show this performance without the aid of CRC. Hence LDPC performance can be further enhanced by using a CRC. On the other hand, polar codes have the benefit of not having an error floor compared to LDPC and turbo, both of which have error floors. However, to achieve the optimal performance of polar codes, code construction should be done based on the channel. Hence, polar codes are not yet versatile. Further research should be conducted to achieve channel independent code design.

Although SC decoder of polar codes shows the lowest complexity, CRC aided SCL decoder exceeds the complexity of LDPC codes and turbo codes. Actual costs of SLC decoder is uncertain due to lack of implementations. There are many other factors

to be considered when choosing a coding scheme, such as latency for encoding and decoding, energy efficiency, and area efficiency. In current implementations, LDPC codes show relatively good performance in both area and energy efficiency. Turbo codes consume highest energy per bit and has a very low area efficiency. Turbo codes have good energy efficiency but low area efficiency. Exact area and energy efficiency of SCL decoder of polar codes are not known yet due to lack of implementations. By comparing code performance in AWGN and fading channels, it can be seen that fading channel performance follows the same trend as the AWGN channel performance.

7. RECOMMENDATIONS FOR FUTURE

Performance of single carrier waveforms was analyzed in AWGN, correlated, and practical channel models in Chapter 2. However,the effect of hardware imperfections also need to be taken into account in order to get a more practical performance. Furthermore, other performance aspects such as sum rate, efficient power allocation techniques should also be investigated.

Turbo, LDPC and Polar codes were evaluated in terms of BLER/BER performance and computational complexity in Chapter 3. We considered max-log-MAP, Offset-min-sum and CRCA-SCL decoding algorithms respectively for each coding scheme. In addition, other efficient decoding algorithms need to be taken into account. For example, sequential decoding algorithm for polar decoding should be compared with SCL decoder to choose an efficient decoding scheme for polar codes. Also, polar codes need to be researched further in the areas of performance of higher order modulation schemes, design of interleavers to be used with polar codes, and cost of hardware implementation.

8. REFERENCES

[1] N. Rajatheva, S. Suyama, W. Zirwas, L. Thiele, G. Fodor, A. Tolli, E. De Carvalho, J. H. Sorensen, "Massive multiple input multiple output (MIMO) systems," in *5G Mobile and Wireless Communications Technology, Cambridge University Press,* Chapter 8, pp. 208-247, June 2016.

[2] "5G Use Cases and Requirements White Paper," in *Nokia White Paper,* July 2014, [online]. Available: `http://resources.alcatel-lucent.com/asset/200010`.

[3] "The Road to 5G: Drivers, Applications, Requirements and Technical Development," in *Global Mobile Suppliers Association(GSA) Executive Report,* November 2015, [online]. Avalable: `http://www.huawei.com/minisite/5g/img/GSA_the_Road_to_5G.pdf`.

[4] J.G. Andrews, S. Buzzi, W. Choi, S.V. Hanly, A. Lozano, A.C.K. Soong, and J.C. Zhang, "What Will 5G Be?," in *IEEE Journal on Selected Areas in Communications,* vol. 32, no. 6, pp. 1065-1082, June 2014.

[5] T. Jiang and Y. Wu, "An Overview: Peak-to-Average Power Ratio Reduction Techniques for OFDM Signals," in *IEEE Transactions on Broadcasting* , vol. 54,no. 2, pp. 257-268, 2008.

[6] S. Shepherd, J. Orriss, and S. Barton, “Asymptotic limits in peak envelope power reduction by redundant coding in orthogonal frequency division multiplex modulation,” in *IEEE Transactions in Communications,* vol. 46, no. 1, pp. 5–10, Jan. 1998.

[7] X. Li and L. J. Cimini, "Effects of Clipping and Filtering on the performance of OFDM," in *IEEE Electronic Letters,* vol. 2, no. 5, pp. 131-133, 1998.

[8] J. Armstrong, "Peak-to-Average power reduction for OFDM by repeated clipping and frequency domain filtering," in *IEEE Electronic Letters,* vol. 38, no. 5, pp. 246-247, February 2002.

[9] A. E. Jones, T. A. Wilkinson, S. K. Barton, "Block coding scheme for reduction of peak to mean envelope power ratio of multicarrier transmission schemes," in *IEEE Electronics Letters,* vol. 30, no. 25, pp. 2098-2099, 1994.

[10] D. Wulich, “Reduction of peak to mean ratio of multicarrier modulation using cyclic coding,” in *IEE Electronics Letters,* vol. 32, no. 29, pp. 432-433, Feb. 1996.

[11] T. Jiang and G. Zhu, "Complement block coding for reduction in peak-to-average power ratio of OFDM signals" in *IEEE Communications Magazine,* vol. 43,no. 9, pp. s17-s22, September 2005.

[12] S. H. Muller and J. B. Huber, "OFDM with reduced peak-to-average power ratio by optimum combination of partial transmit sequences,” in *IEE Electronics Letters,* vol. 33, no. 5, pp. 36-69, Feb. 1997.

[13] L. Yang, R.S. Chen,Y. M. Siu,K. Soo, “PAPR reduction of an OFDM signal by use of PTS with low computational complexity,” in *IEEE Transactions on Broadcasting,* vol. 52, no. 1, pp. 83–86, Mar. 2006.

[14] J. Tellado,“Peak to Average Power Ratio Reduction for Multicarrier Modulation,” in *PhD thesis,University of Stanford,* 1999.

[15] T. Jiang,Y. Yang,Y. Song, "Exponential companding technique for PAPR reduction in OFDM systems," in *IEEE Transactions on Broadcasting,* vol. 51, no. 2, pp. 244-248, June 2005.

[16] H. Gacanin, S. Takaoka, F. Adachi, "Generalized OFDM for bridging between OFDM and single-carrier transmission," in *The Ninth International Conference on Communication Systems, ICCS 2004,* pp. 145-149, Sept. 2004.

[17] R. W. Bauml, R. F. H. Fisher,J. B. Huber, “Reducing the Peak-to-Average Power Ratio of Multicarrier Modulation by Selected Mapping” in *IEE Electronics Letters,* vol. 32, no. 22, pp. 2056-2057, Oct.1996.

[18] A. A. Abouda, "PAPR reduction of OFDM signal using turbo coding and selective mapping," in *Proceedings of the 6th Nordic Signal Processing Symposium, NORSIG 2004,* pp. 248-251, June 2004.

[19] H. Gamage, N. Rajatheva and M. Latva-aho, "High PAPR Sequence Scrambling for Reducing OFDM Peak-to-Average Power Ratio" in *European Wireless 2016; 22th European Wireless Conference,* Oulu, April 2016.

[20] "3GPP Contributions[Online]". Available: `http://www.3gpp.org/DynaReport/TDocExMtg--R1-86--31663.htm`.

[21] Verizon, "Verizon 5G Technical Forum," 2016, [Online]. Available: `http://www.5gtf.org`.

[22] M. Tercero, P. Wrycza, A. Amah, J. Widmer, M. Fresia, V. Frascolla, J.Lorca, T. Svensson, M. Hamon, S. D. Roblot, A. Vijay, M. Peter, V. Sgardoni, M. Hunukumbure, J. Luo and N. Vucic, "5G systems: The mmMAGIC project perspective on use cases and challenges between 6–100 GHz," in *IEEE Conference on Wireless Communications and Networking WCNC,* April 2016.

[23] T. L. Marzetta, "Noncooperative Cellular Wireless with Unlimited Numbers of Base Station Antennas," in *IEEE Transactions on Communications,* vol. 9, no. 11, pp. 3590-3600, November 2010.

[24] A. Roivainen, P. Kyösti, C. F. Dias, V. Hovinen, N. Tervo, M. Sonkki, and M. Latva-aho, "Geometry-Based Stochastic Channel Model Parametrization for Urban Small Cells at 10 GHz," in *IEEE Transactions on Antennas and Propagation,* under revision, May 2016.

[25] A. Roivainen, C. F. Dias, N. Tervo, and M. Latva-aho, "Geometry-Based Stochastic Channel Model for Two-Story Lobby Environment at 10 GHz," in *IEEE Transactions on Antennas and Propagation,* vol. 64, no. 9, pp. 3990-4003, Sept. 2016.

[26] P. Yang et al., "Single-Carrier SM-MIMO: A Promising Design for Broadband Large-Scale Antenna Systems," in *IEEE Communications Surveys and Tutorials,* vol. 18, no. 3, pp. 1687-1716, Third Quarter 2016.

[27] A. Pitarokoilis, S. K. Mohammed and E. J. Larsson, "On the Optimality of Single-Carrier Transmission in Large-Scale Antenna Systems," in *IEEE Wireless Communications Letters,* vol. 1, no. 4, pp. 276-279, Aug. 2012.

[28] Y. Sheng, Z. Tan and G. Ye Li, "Single-Carrier Modulation with ML Equalization for Large-Scale Antenna Systems over Rician Fading Channels," in *IEEE Conference on Acoustic, Speech and Signal Processing, ICASSP,* pp. 5759-5763, September 2014.

[29] Y. Liu, G. Ye Li, Z. Tan and D. Qiao, "Performance Analysis of Single-Carrier Modulation with Correlated Large-Scale Antennas" [Online]. Available: `https://arxiv.org/pdf/1508.00109`.

[30] Yu Zhu, Peng Zhe, Hong Zhou and D. Huang, "Robust Single Carrier Frequency Domain Equalization with Imperfect Channel Knowledge," in *IEEE Transactions on Wireless Communications,* vol. 15, no. 9, pp. 6092-6103, September 2016.

Turbo

[31] C. Berrou, A. Glavieux and P. Thitimajshima, "Near Shannon limit error-correcting coding and decoding: Turbo-codes," in *IEEE International Conference on Communications,* 1993.

[32] A. Goldsmith, "Chapter 8: Coding for wireless channels," in *Wireless Communications,* Cambridge University Press, 2005.

[33] R.G. Gallarger, "Low Density Parity Check codes," in *IRE Transactions on Information Theory,* 1962.

[34] D.J.C. MacKay and R.M. Neal, "Near Shannon limit performance of low density parity check codes," in *Electronic Letters,* Vol. 33, No. 6, March 1997.

[35] E. Arikan, "Channel Polarization: A Method for Constructing Capacity-Achieving Codes for Symmetric Binary-Input Memoryless Channels," in *IEEE Transactions on Information Theory,* vol. 55, no. 7, pp. 3051-3073, July 2009.

[36] M. Sybis, K. Wesolowski, K. Jayasinghe, V. Venkatasubramanian, and V. Vukadionovic, "Channel coding for ultra-reliable low-latency communication for 5G systems," in *IEEE Vehicular Technology Conference(VTC Fall 2016),* 2016.

[37] H. Gamage, N. Rajatheva and M. Latva-aho, "Channel Coding for Enhanced Mobile Broadband Communication in 5G Systems," in submitted to *European Conference on Networking and Communications,* 2017.

[38] ETSI, "Evolved Universal Terrestrial Radio Access (E-UTRA) Multiplexing and Channel Coding," in *3GPP Technical specification,* version 12.6.0, Release 12.

[39] I. Tal and A. Vardy, "List Decoding of Polar Codes," in *IEEE Transactions on Information Theory*, vol. 61, no. 5, pp. 2213-2226, May 2015.

[40] H. Vangala, E. Viterbo and Y. Hong , "A Comparative Study of Polar Code Constructions for the AWGN Channel," in *IEEE Transactions on Information Theory,* vol. 61, no. 5, pp. 2213-2226, Jan. 2015.

[41] C. Studer, C. Benkeser, S. Belfanti, and Q. Huang, "Design and Implementation of a Parallel Turbo-Decoder ASIC for 3GPP-LTE," in *IEEE Journal of Solid-State Circuits,* 2011.

[42] A.Bravo-Santos, "Polar Codes for the Rayleigh Fading Channel," in *IEEE Communication Letters,* vol. 17, issue. 12, December 2013.

[43] S. Le Goff, A. Glavieux and C. Berrou, "Turbo-codes and high spectral efficiency modulation," in *IEEE International Conference in Communications,* vol. 2, pp. 645-649, May 1994.

[44] R. Yazdani and M. Ardakani, "Optimum Linear LLR Calculation for Iterative Decoding on Fading Channels," in *IEEE International Symposium on Information Theory (ISIT),* June 2007.